© 2015. Published by The Company of Biologists Ltd | Journal of Cell Science (2015) 128, 2070-2084 doi:10.1242/jcs.161810

RESEARCH ARTICLE

The *Drosophila* fragile X mental retardation protein participates in the piRNA pathway

Maria Pia Bozzetti[1,§,¶], Valeria Specchia[1,§], Pierre B. Cattenoz[2,3,4,5], Pietro Laneve[2,3,4,5,*], Annamaria Geusa[1,2,3,4,5], H. Bahar Sahin[2,3,4,5,‡], Silvia Di Tommaso[1], Antonella Friscini[1], Serafina Massari[1], Celine Diebold[2,3,4,5] and Angela Giangrande[2,3,4,5,¶]

ABSTRACT

RNA metabolism controls multiple biological processes, and a specific class of small RNAs, called piRNAs, act as genome guardians by silencing the expression of transposons and repetitive sequences in the gonads. Defects in the piRNA pathway affect genome integrity and fertility. The possible implications in physiopathological mechanisms of human diseases have made the piRNA pathway the object of intense investigation, and recent work suggests that there is a role for this pathway in somatic processes including synaptic plasticity. The RNA-binding fragile X mental retardation protein (FMRP, also known as FMR1) controls translation and its loss triggers the most frequent syndromic form of mental retardation as well as gonadal defects in humans. Here, we demonstrate for the first time that germline, as well as somatic expression, of *Drosophila* Fmr1 (denoted dFmr1), the *Drosophila* ortholog of FMRP, are necessary in a pathway mediated by piRNAs. Moreover, *dFmr1* interacts genetically and biochemically with Aubergine, an Argonaute protein and a key player in this pathway. Our data provide novel perspectives for understanding the phenotypes observed in Fragile X patients and support the view that piRNAs might be at work in the nervous system.

KEY WORDS: dFmr1, *Drosophila*, piRNAs, Transposable elements, *aubergine*, *crystal–Stellate*

INTRODUCTION

Mutations in the fragile X mental retardation protein (FMRP, also known as FMR1) cause Fragile X syndrome, which entails cognitive and gonadal defects in humans (de Roodt et al., 2009; Jin et al., 2004a; Jin and Warren, 2000; Tamanini et al., 1997; Verkerk et al., 1991). The members of the FMRP family act in the control of RNA translation in the nervous system (Epstein et al., 2009; Jin et al., 2004a; Jin et al., 2004b) and in the ovaries (Epstein et al., 2009). More interestingly, these proteins have been reported to associate and interact with components of the RNA-induced silencing complex (RISC) including AGO1 and AGO2, two members of the Argonaute protein family, which mediate post-transcriptional control through small RNAs. Thus, RNA interference (RNAi)-mediated pathways are known to be involved in the translational regulation mediated by FMRP (Caudy et al., 2002; Ishizuka et al., 2002; Jin et al., 2004b).

AGO1 is predominantly involved in the microRNA (miRNA)-mediated silencing and AGO2 in the small interfering RNA (siRNA)-mediated silencing (Aravin et al., 2001; Czech and Hannon, 2011). The PIWI subclade of Argonaute proteins, which includes *Drosophila* Aubergine (Aub), AGO3 and Piwi, interacts with the so-called piRNAs and silences transposable as well as repetitive elements, thereby protecting the genome from instability. The piRNA-mediated pathway was first discovered in the germline (Carmell et al., 2002; Gunawardane et al., 2007; Ishizu et al., 2012; Krusiński et al., 2008; Laskowski and Hillhouse, 2008; Senti and Brennecke, 2010; Thomson and Lin, 2009; Vagin et al., 2006 and references therein) and more recently in the nervous system (Baillie et al., 2011; Brennecke et al., 2008; Lee et al., 2012; Lee et al., 2011; Lukic and Chen, 2011; Perrat et al., 2013; Plaisant et al., 2008; Rajasethupathy et al., 2012; Reilly et al., 2013; Sato and Siomi, 2010; Specchia et al., 2010; Thomas et al., 2012). Although recent high throughput analyses have identified an increasing number of piRNA-related genes (Czech et al., 2013; Handler et al., 2013; Muerdter et al., 2013), the molecular mechanisms underlying the piRNA pathway have not been fully elucidated yet. Furthermore, although the different classes of small RNA display specific features, there seems to be no clear line separating them (Förstemann et al., 2007). Indeed, AGO1 and AGO2 can compete for binding with miRNAs (Laskowitz and Warner, 2008) and ectopic expression of Aub in the soma competes for the siRNA pathway mediated by AGO2 (Specchia et al., 2008). Such promiscuity, the known role of the FMRP protein family in small RNA metabolism (Ascano et al., 2012a; Ascano et al., 2012b; Epstein et al., 2009; Ishizu et al., 2012) and the presence of transposons in the nervous system, a key target tissue of the FMRP protein family (Lee et al., 2011; Perrat et al., 2013), prompted us to hypothesize the involvement of the *Drosophila* ortholog dFmr1 protein in the piRNA pathway.

One of the most known piRNA-mediated pathways in *Drosophila* is the one regulating the interaction between *crystal* [*cry*, also known as *Su(Ste)*] and *Stellate* (*Ste*, also known as *SteXh*) (Bozzetti et al., 2012; Bozzetti et al., 1995; Li et al., 2009; Nagao et al., 2010; Vagin et al., 2006). In wild-type (wt) testes, piRNAs mainly produced by the *cry* locus silence the expression of the *Ste* RNA. Males lacking this locus exhibit meiotic defects in chromosome condensation and segregation as well as crystalline aggregates, due to the production of the Ste protein (Bozzetti et al., 2012; Bozzetti et al., 1995; Palumbo et al., 1994; Tritto et al., 2003). All of the so far identified *cry–Ste* modifiers are involved in the piRNA pathway and, beyond the crystalline aggregates in spermatocytes, they also share sterility and germline activation of transposable elements (Li et al., 2009; Nagao et al., 2010; Specchia et al., 2010; Vagin et al., 2006; Zhang et al., 2011).

[1]Dipartimento di Scienze e Tecnologie Biologiche ed Ambientali (DiSTeBA) – University of Salento, 73100 Lecce, Italy. [2]Institut de Génétique et de Biologie Moléculaire et Cellulaire, 67404 Illkirch, France. [3]Centre National de la Recherche Scientifique, UMR7104, 67404 Illkirch, France. [4]Institut National de la Santé et de la Recherche Médicale, U964, 67404 Illkirch, France. [5]Université de Strasbourg, Illkirch, France.
*Present address: Center for Life NanoScience, Istituto Italiano di Tecnologia, Rome, Italy. ‡Present address: Department of Bioinformatics and Genetics – Kadir Has University, Cibali – Fatih, Istanbul.
§These authors contributed equally to this work

¶Authors for correspondence (maria.bozzetti@unisalento.it; angela@igbmc.fr)

Received 15 August 2014; Accepted 10 April 2015

Journal of Cell Science

Journal of Cell Science (2015) 128, 2070-2084 doi:10.1242/jcs.161810

Here, we provide clear evidence that *Drosophila Fmr1* (denoted *dFmr1*) acts in the piRNA pathway. First, *dFmr1* loss-of-function (LOF) mutations exhibit crystalline aggregates in spermatocytes, and derepression of transposable elements in testes and ovaries as well as fertility defects. Second, dFmr1 overlaps and interacts genetically as well as biochemically with Aub. Surprisingly, dFmr1 is required both in the germline and in the somatic compartments of the testis to control the piRNA pathway. The present work provides novel perspectives in the field of RNA metabolism and broadens our understanding of the physiopathological mechanisms underlying the Fragile X syndrome.

RESULTS

dFmr1 acts in the piRNA pathway

The piRNA pathway silences transposons and repetitive elements, and the *cry–Ste* system provides a faithful readout to study silencing of the latter. As a first attempt to assess the role of dFmr1 in the pathway, we analyzed *dFmr1* testes. $dFmr1^{\Delta 50}$, $dFmr1^{\Delta 113}$ homozygous and $dFmr1^{\Delta 113}/dFmr1^{\Delta 50}$ testes (referred to as transheterozygous throughout the text) exhibit crystals, a phenotype that is absent in wt animals (Fig. 1A–C,G). Interestingly, $dFmr1^{\Delta 113}/+$ testes also show crystals, whereas $dFmr1^{\Delta 50}/+$ testes do not (Fig. 1D,E). To clarify the different phenotypes of the mutations that were considered to be nulls, we performed western blot analyses on adult testes and on larvae and found that $dFmr1^{\Delta 50}$ and $dFmr1^{\Delta 113}$ represent a hypomorphic and a null allele, respectively (Fig. 1H; supplementary material Fig. S1), in line with the described size of the deletions, which include the first coding exon in the case of $dFmr1^{\Delta 50}$ and the first two coding exons in the case of $dFmr1^{\Delta 113}$ (Zhang et al., 2001; Zhang et al., 2004). This likely accounts for the almost complete lethality of homozygous $dFmr1^{\Delta 113}$ (but not $dFmr1^{\Delta 50}$) flies in our growing conditions.

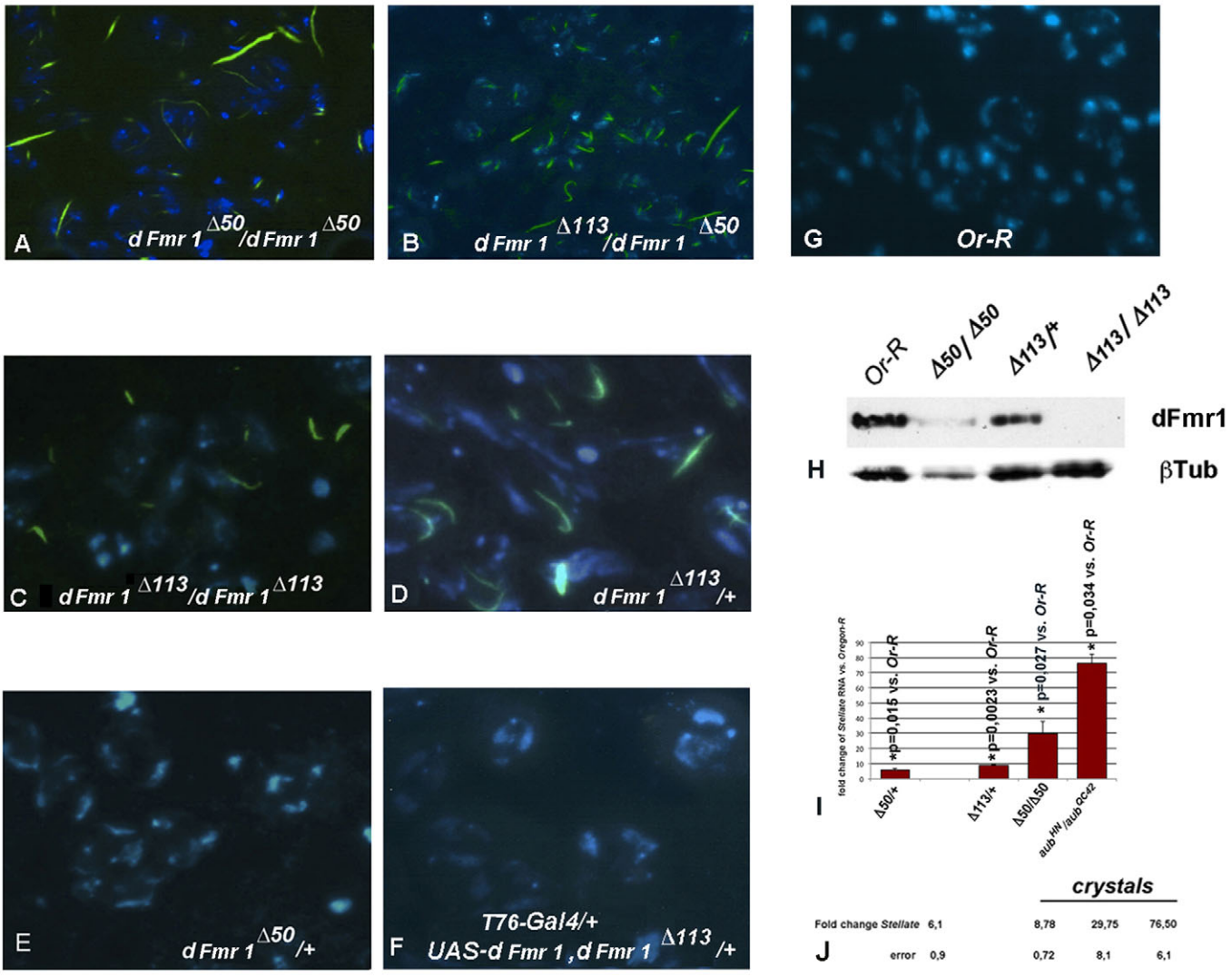

Fig. 1. *dFmr1* adult testes exhibit *cry–Ste* deregulation. (A–G) Crystal phenotype in the indicated genotypes analyzed by epifluorescence microscope; anti-Ste labeling is in green, DAPI in blue. *T76-Gal4* is considered as a germline driver (Hrdlicka et al., 2002; Arya et al., 2006). The images were taken with a 40× magnification objective. All of the 'crystal' images were obtained in the same conditions. (H) Western blot analysis with anti-dFmr1 antibody on protein extracts from of third-instar larvae of the indicated genotypes. The $dFmr1^{\Delta 50}$mutation triggers the expression of a residual protein that is 17 amino acids shorter than the wt protein, whereas the $dFmr1^{\Delta 113}$mutation results in the complete lack of dFmr1 protein (Reeve et al., 2005). The lower panels show the anti-β-tubulin loading control. (I) qRT-PCR analysis of *Ste* expression in $dFmr1^{\Delta 50}/+$, $dFmr1^{\Delta 113}/+$, $dFmr1^{\Delta 50}/dFmr1^{\Delta 50}$ and aub^{HN}/aub^{QC42} testes, used as a positive control. Data are mean±s.e.m. from four independent experiments. (J) Mean fold changes observed in the above genotypes; errors are calculated as reported in Materials and Methods. *Or-R* (*Oregon-R*) represents the control.

Journal of Cell Science (2015) 128, 2070-2084 doi:10.1242/jcs.161810

Importantly, *dFmr1* expression in testes driven by the *T76* driver (Arya et al., 2006; Hrdlicka et al., 2002) rescues the 'crystal' phenotype of $dFmr1^{\Delta 113}$ heterozygous and homozygous flies as well as the lethality of the homozygous flies (Fig. 1F, *T76-Gal4/+;UAS-dFmr1,* $dFmr1^{\Delta 113}$/+; and data not shown), confirming that these defects depend on the *dFmr1* mutation. Thus, *dFmr1* regulates the *cry–Ste* interaction. For the rest of our analysis, we used $dFmr1^{\Delta 113}$ heterozygous flies whenever possible but always retested the results using homozygous $dFmr1^{\Delta 50}$ or transheterozygous flies.

The presence of crystals suggests a derepression of the *Ste* locus, as previously found in testes mutant for Aub (Schmidt et al., 1999; Specchia et al., 2008), a known modifier of the *cry–Ste* interaction (Fig. 1I,J). Compared to controls, *dFmr1* mutant animals show an increase of *Ste* RNA expression, which we assessed by quantitative real-time PCR (qRT-PCR) assays. $dFmr1^{\Delta 50}$ homozygous animals show a stronger increase (Fig. 1I,J; 29.7 fold) than that observed in $dFmr1^{\Delta 113}$ heterozygous testes (8.7 fold) and, as expected, $dFmr1^{\Delta 50}$ heterozygous animals show the lowest increase of *Ste* RNA levels (6.1 fold). At least an eightfold increase of *Ste* RNA expression is required to produce crystals (Specchia et al., 2010), likely explaining the absence of the crystalline structures in $dFmr1^{\Delta 50}$ heterozygous testes.

Given that the decrease in *cry*-specific piRNAs induces *Ste* RNA expression and crystal formation (Aravin et al., 2003; Aravin et al., 2001; Nagao et al., 2010; Specchia et al., 2010), we analyzed the expression of two of the most abundant *cry*-specific piRNAs in *dFmr1* mutant testes by northern blotting and by qRT-PCR, and we found that they decrease compared to what was observed in controls ('*crystal*' and '*rasi4*'; see Materials and Methods). $dFmr1^{\Delta 50}$ homozygous and transheterozygous testes display the most severe reduction, $dFmr1^{\Delta 113}$ heterozygous testes are less affected and $dFmr1^{\Delta 50}$ heterozygous testes result was only significantly different for the qRT-PCR analysis (Fig. 2A,C,D,F and data not shown). Importantly, the levels of both *cry*-specific piRNAs are rescued upon reintroducing *dFmr1* expression in mutant testes (Fig. 2B,E). To assess whether the piRNA pathway affecting transposons is also affected by dFmr1, we next tested the expression of a piRNA specific to the *R1* transposable element. In line with the crystal phenotype, we observed a severe reduction of the levels of this piRNA in $dFmr1^{\Delta 50}$ homozygous with respect to those found in $dFmr1^{\Delta 50}$ heterozygous testes (Fig. 2C,D); $dFmr1^{\Delta 113}$ heterozygous animals harbor an intermediate phenotype. Finally, we found no evidence for enhanced levels of piRNA precursors.

We also analyzed transposable element silencing. It is generally accepted that, in the fly gonads, the 'primary piRNA pathway' predominantly controls the levels of piRNAs specific to the so-called 'somatic' transposable elements and involves Piwi, whereas the secondary piRNA pathway involves AGO3 and Aub, requires a piRNA amplification loop and controls the levels of piRNAs specific to the 'germline' transposable elements (Brennecke et al., 2007; Li et al., 2009; Malone et al., 2009; Nagao et al., 2010). Amongst the 'germline' group of transposons, we analyzed *roo*, *I* and *R1*; amongst the 'somatic' group, we analyzed *ZAM*, *gypsy*, *412* and *springer*. The levels of the transcripts of the 'germline' transposons clearly increase in $dFmr1^{\Delta 50}$ homozygous testes compared to those observed in $dFmr1^{\Delta 50}$ heterozygous ones, which were taken as controls (Fig. 2G, left part). Specific 'somatic' transposons are also affected (*ZAM* levels increase moderately, whereas *gypsy*, *412* and *springer* levels do not; Fig. 2G, right part). Germline and somatic transposons are expressed at almost wt levels in $dFmr1^{\Delta 113}$ heterozygous testes (Fig. 2H), confirming that the phenotype of these animals is weaker than that of $dFmr1^{\Delta 50}$ homozygous ones.

Taken together, these results suggest that *dFmr1* behaves as a bona fide member of the piRNA pathway. It controls the levels of *cry*-specific piRNAs as well as those of piRNAs related to 'germline' and 'somatic' transposons in testes, hence affecting the expression and/or movement of these transposons.

dFmr1 controls fertility in males and females

The movement of transposable elements is one of the molecular causes of DNA instability and sterility (Brennecke et al., 2007; Khurana et al., 2011) and most genes involved in the piRNA pathway identified so far, including all the *cry–Ste* modifiers, are partially or completely male-sterile (Handler et al., 2013; Li et al., 2009; Muerdter et al., 2013; Pane et al., 2007; Perrat et al., 2013; Schmidt et al., 1999; Specchia et al., 2008; Specchia and Bozzetti, 2009; Specchia et al., 2010; Stapleton et al., 2001; Tomari et al., 2004; Vagin et al., 2006). $dFmr1^{\Delta 50}$ homo- and transheterozygous males are completely sterile [Fig. 2I, versus w^{1118} ; similar results were obtained upon comparison with *Oregon R* (*Or-R*) flies, data not shown]. Importantly, the fertility defects of (heterozygous, transheterozygous and homozygous) *dFmr1* mutant males are significantly rescued upon reintroducing *dFmr1* expression (Fig. 2I, *T76-Gal4/+;UAS-dFmr1,* $dFmr1^{\Delta 113}/dFmr1^{\Delta 50}$ and data not shown).

The so far identified mutations of the piRNA pathway also exhibit female fertility defects associated with transposon activation (Czech et al., 2013; Ishizu et al., 2012). We therefore analyzed $dFmr1^{\Delta 50}$ homozygous female gonads for the activation of the same transposons as those analyzed in males and found that the levels of *I, roo* and *R1* transcripts increase even more than in testes (Fig. 2J, left part). As in males, the somatic transposons behave differently from one another: *ZAM* and *gypsy* are activated at a high rate, whereas *springer* and *412* remain almost at the same level as in wt animals (Fig. 2J, right part). Accordingly, the fertility of *dFmr1* mutant females is significantly reduced ($dFmr1^{\Delta 50}$ heterozygous, transheterozygous and homozygous females, Fig. 2K; we obtained similar results with *Or-R*, data not shown). The fertility of $dFmr1^{\Delta 50}$ heterozygous and homozygous females is rescued upon reintroducing *dFmr1* expression (data not shown).

In summary, *dFmr1* affects transposon activation and fertility in males and in females.

dFmr1 and Aub colocalize in testis and ovaries and interact biochemically

To gain insights on the mode of action of dFmr1, we analyzed its profile of expression in the adult testes. dFmr1 is expressed in the germ cells, as confirmed by double labeling using the anti-Vasa germline-specific marker (Lasko, 2013 and references therein; supplementary material Fig. S2). It widely accumulates in the cytoplasm, as expected from its described role in translational control, and it overlaps with Vasa in the nuage, a perinuclear compartment where the other components of the piRNA pathway accumulate (Anand and Kai, 2012; Ishizu et al., 2012; Pek et al., 2012). A prominent colocalization occurs at the level of the piNG bodies, structures in which piRNA components are located and perform their function (Kibanov et al., 2011) (supplementary material Fig. S2C–H, see arrowheads).

Aub constitutes one of the best-known players of the piRNA pathway and its loss triggers the formation of crystals in testes (Schmidt et al., 1999) (Fig. 1I,J). As for the other proteins involved in the piRNA pathway, Aub is specifically expressed in the

Journal of Cell Science

Journal of Cell Science (2015) 128, 2070-2084 doi:10.1242/jcs.161810

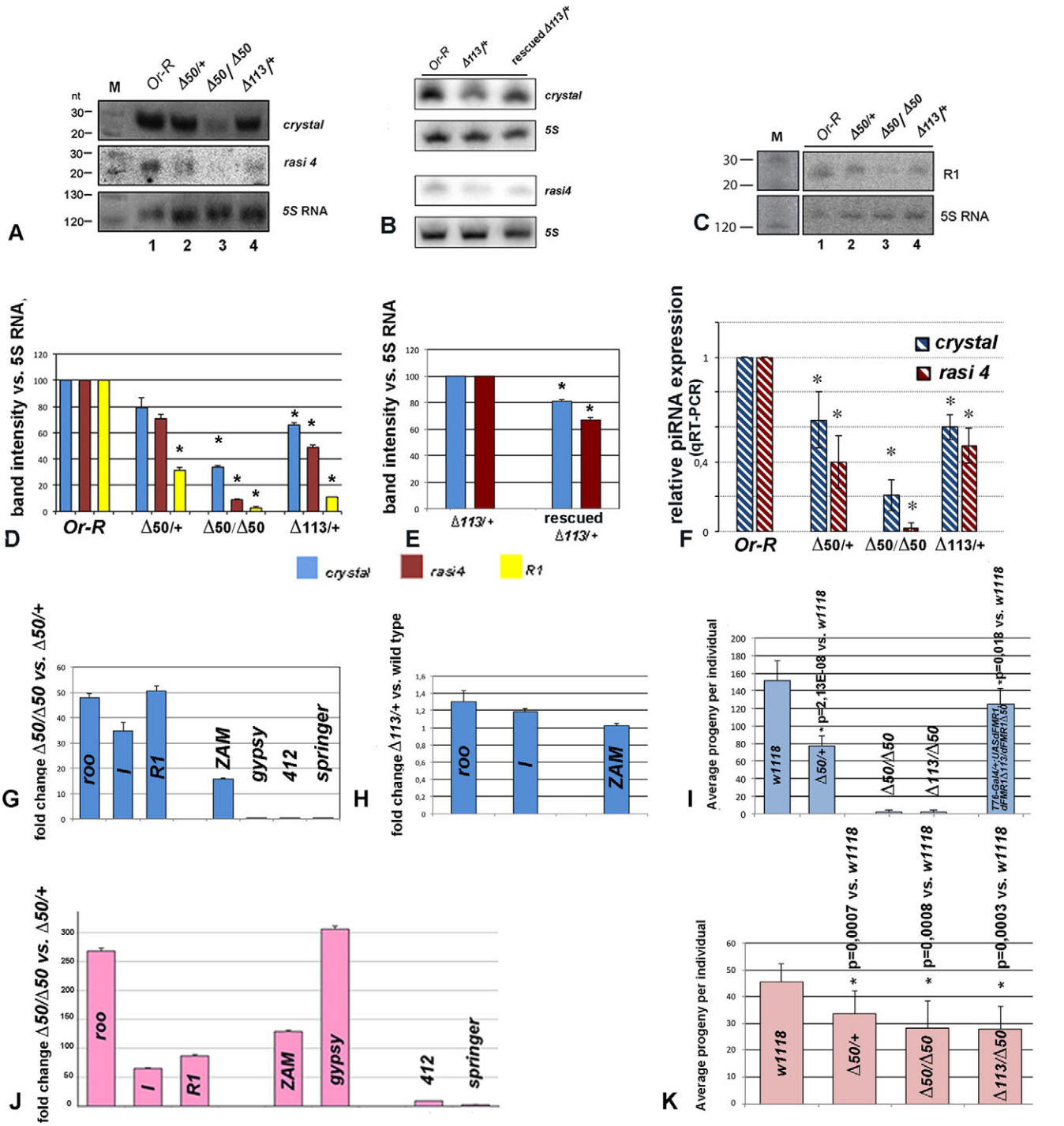

Fig. 2. dFmr1 belongs to the piRNA pathway. (A,B) Northern blot analyses on enriched small RNA extracts from the indicated genotypes probed with two different *cry*-specific piRNAs (*crystal* and *rasi4*). (C) Northern blot analyses from the same genotypes as in A probed with a R1-specific piRNA. In both cases, 5S RNA was used as a loading control. (D) Quantification (mean±s.d.) of the northern blot analyses reported in A. (E) Quantification (mean±s.d.) of the northern blot analyses reported in B. Rescued *Δ113*/+ corresponds to *T76-Gal4*/+, *UAS-dFmr1, dFMR1*$^{\Delta 113}$ /+; *n*=2. (F) qRT-PCR analysis (mean±s.d.) of the indicated genotypes on two different *cry*-specific piRNAs (*crystal* and *rasi4*). **P*<0.05 compared with the control. (G) qRT-PCR analysis on transposon expression in *dFMR1*$^{\Delta 50}$ homozygous versus heterozygous, control testes (the left columns show the germline transposons *roo*, *I* and *R1*, and the right-hand columns show the somatic transposons *ZAM*, *gypsy*, *412* and *springer*). Data are mean±s.e.m. from three independent experiments. (H) qRT-PCR analysis (error bars have been calculated as described in the Materials and Methods) on transposon expression in *dFMR1*$^{\Delta 113}$ heterozygous versus wt testes. (I) Male fertility in the mentioned genotypes. Results are mean±s.d., *n*=3. (J) qRT-PCR analysis (error bars have been calculated as described in the Materials and Methods) on transposon expression in ovaries, genotypes as in G. (K) Female fertility (mean±s.d., *n*=3) in the mentioned genotypes.

germline, and localizes to the 'nuage', accumulating preferentially at the piNG bodies (Kibanov et al., 2011; Li et al., 2009; Nagao et al., 2010; Pek et al., 2012; Specchia and Bozzetti, 2009; Zamparini et al., 2011; Zhang et al., 2012; Zhang et al., 2011). Double labeling with anti-Aub and anti-Fmr1 antibodies (Fig. 3A–L) confirms the overlap at the level of the nuage (Fig. 3E–L) and strong

Journal of Cell Science (2015) 128, 2070-2084 doi:10.1242/jcs.161810

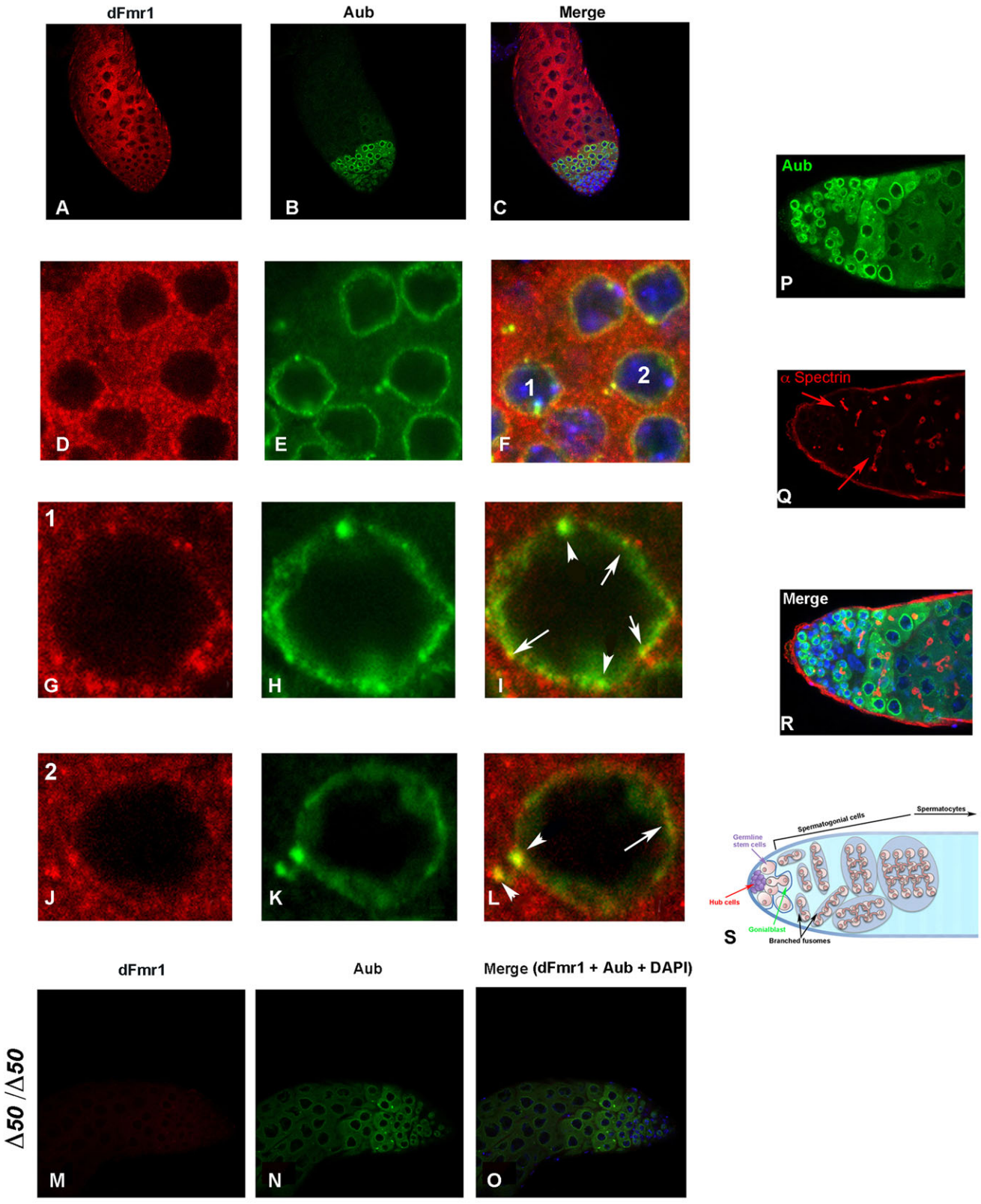

Fig. 3. dFmr1-Aub colocalization in testes and interaction. (A–L) Projections of two confocal sections of a wt testis, labeled with anti-dFmr1 antibody (red, A,D,G,J), anti-Aub antibody (green, B,E,H,K), and the merged image (C,F,I,L). C,F also shows DAPI labeling. (G–I,J–L) Photographic zooms of the cells indicated by 1 and 2 in F, respectively. Arrows indicate dFmr1–Aub colocalization; arrowheads point to the piNG bodies. (M–O) Projections and labeling as above in a *dFmr1*$^{\Delta 50}$ homozygous testis, also showing the DAPI labeling. As expected, no dFmr1 labeling can be detected and the Aub profile does not seem to be altered. (P–R) Confocal projections (five sections) from a wt testis labeled with anti-Aub antibody (green, P) and anti-α-Spectrin antibody (red, Q). Arrows indicate the branched fusomes, the merged image (R) also shows DAPI labeling. (S) Schematic of the apical region of adult wt testis. The images were taken with a 40× magnification objective, and those in D–F are shown magnified 2.5 fold.

Journal of Cell Science (2015) 128, 2070-2084 doi:10.1242/jcs.161810

colocalization in the piNG bodies (Fig. 3G–L). Within the testis, Aub levels are highest in the apical tip (Fig. 3B), which corresponds to the earliest developmental stages. To further characterize Aub distribution throughout the testis, we used anti-Aub antibody staining and a marker for the fusome, a germline structure that changes morphology during germ cell differentiation, being globular in stem cells and gonialblast while branched in spermatogonia (Fig. 3P–R, red arrows in Fig. 3Q and testis schematic in Fig. 3S). The highest levels of Aub occur in stem cells, spermatogonia and possibly early spermatocytes. dFmr1 expression extends to the late stages. Aub expression therefore seems to colocalize with dFmr1 in a specific territory that corresponds to that of the early spermatocytes (Fig. 3A–C). dFmr1 does not seem to affect Aub expression, which still accumulates and localizes properly in $dFmr1^{\Delta 50}$ homozygous testis (Fig. 3M–O).

We also analyzed the expression profile of Aub and dFMR1 in ovaries from wt adults (Fig. 4A–Q). The two proteins colocalize in the germarium, mostly at the position of the stem cells (Fig. 4A–D) and later on they overlap at the nuage of the nurse cells (Fig. 4E–P). By stage 6, the two proteins also colocalize in the oocyte cytoplasm (Fig. 4M–P), which will eventually contain the polar granules, where Aub, dFmr1 and Vasa accumulate (Costa et al., 2005; Hillebrand et al., 2007; Thomson et al., 2008). dFmr1 does not seem to affect Aub expression, which still accumulates and localizes properly in $dFmr1^{\Delta 50}$ homozygous ovaries (Fig. 4R–U).

As a further evidence for a role of dFmr1 in the piRNA pathway, we asked whether the two proteins interact biochemically, as has been shown for dFmr1 and other members of the AGO family (Ishizuka et al., 2002; Jin et al., 2004a; Jin et al., 2004b; Zhang et al., 2004). Aub and dFmr1 cotransfection assays in S2 *Drosophila* cells, which are devoid of Aub, and immunoprecipitation with an anti-dFmr1 antibody revealed the presence of the Aub protein in the immunoprecipitate (Fig. 4V). A GST pulldown assay using a GST–dFmr1 fusion protein and the *in vitro* translated full-length Aub product demonstrates the direct interaction between the two proteins (Fig. 4W).

In summary, Aub and dFmr1 interact biochemically and colocalize in specific territories and cellular compartments of testes and ovaries.

dFmr1 interacts genetically with Aub in the piRNA pathway

The above data prompted us to analyze the genetic interaction between dFmr1 and Aub. First, we asked whether altering the levels of Aub modifies the effects of dFmr1 loss. Germline Aub overexpression rescues the *dFmr1*-mediated crystal phenotype showing that the two proteins work in the same pathway and act in the same direction (Table 1, genotypes 1–3). The data also suggest that Aub might act downstream of dFmr1. This was confirmed by doing the reverse experiment: dFmr1 overexpression (Table 1, genotypes 4,5) cannot rescue the crystal phenotype triggered by the *aub* knockdown (KD) (Table 1, genotypes 6,7). Finally, we analyzed the crystal phenotype of double heterozygous flies for dFmr1 and different Aub alleles. aub^{HN} and aub^{QC42} are considered as strong hypomorphs that do not exhibit crystals in heterozygous testes but do so in transheterozygous conditions (Table 1, genotypes 9–11). As predicted from the mutant phenotypes of the single genes, aub^{HN}/+; *dFmr1*/+ and aub^{QC42}/+; *dFmr1*/+ flies exhibit crystals (Table 1, genotypes 12,13; Fig. 5A). We then analyzed aub^{sting} testes, which exhibit crystals in transheterozygous conditions with aub^{HN} and aub^{QC42} and not in heterozygous conditions, as the two other alleles (Table 1, genotypes 14–16). aub^{sting} homozygous animals are viable and also present the crystal phenotype (Table 1, genotype 17). Strikingly, aub^{sting}/+; *dFmr1*/+ flies do not exhibit crystals (Table 1, genotype 18; Fig. 5B). Moreover, aub^{sting}/+ rescues the other phenotypes observed in *dFmr1* mutant animals as well, namely, it reduces the expression of the *Ste* RNA transcript and that of transposable elements (supplementary material Table S1). Furthermore, aub^{sting}/+ rescues the male fertility defects linked to $dFmr1^{\Delta 113}$ heterozygous, transheterozygous and homozygous conditions (Fig. 5C; data not shown). Finally, aub^{sting}/+ animals that are homozygous mutant for *dFmr1* show no crystals and aub^{sting}/+; $dFmr1^{\Delta 113}/dFmr1^{\Delta 113}$ animals are fully viable (Table 1, genotypes 19,20).

Similar results were found in females, that is, aub^{sting}/+ reduces the expression of transposable elements observed in homozygous $dFmr1^{\Delta 50}$ ovaries (data not shown) and rescues the fertility defects observed in homozygous and heterozygous $dFmr1^{\Delta 113}$ females (Fig. 5D). Finally, aub^{sting}/+ rescues $dFmr1^{\Delta 113}/dFmr1^{\Delta 113}$ induced lethality in females as well.

aub^{sting} was previously shown to trigger ectopic Aub expression in somatic adult tissues (Specchia et al., 2008) and should be therefore considered as a neomorph in these territories. Given the known germline requirement of the piRNA pathway linked to the *cry–Ste* system, the rescue data with the aub^{sting} allele were quite surprising, prompting us to ask whether, in this allele, Aub is ectopically expressed in the somatic compartment of the gonad and whether the piRNA-mediated *Ste* silencing also has a somatic requirement.

Western blot analyses showed that the Aub protein is not detected in aub^{HN}/aub^{QC42} flies but is present at low levels in aub^{sting} animals (Fig. 6A). Immunolabeling assays clarified these data: aub^{sting} testes show reduced overall levels of Aub in the germline and high levels in the hub, a somatic territory normally devoid of Aub and in direct contact with germ cells (Fig. 6B,E). This was further validated by the colocalization of Aub and the hub marker E-Cadherin in the aub^{sting} testes (Fig. 6B–G). This result suggested that the piRNA pathway regulating *cry-Ste* also has a somatic requirement. We hence specifically expressed Aub in the hub (*upd-Gal4*) and found that this indeed rescues the *dFmr1*-mediated crystal phenotype (Table 1, genotype 8). Thus, the neomorphic behavior of the aub^{sting} mutation (loss of function in the germline and gain of function in the hub) likely accounts for the allele-specific interaction observed with *dFmr1*. In line with this finding, dFmr1 is also expressed in the hub (Fig. 6H–J). Thus, the aub^{sting} allele made it possible to reveal a somatic requirement of the piRNA-mediated *cry-Ste* regulation in the testis.

dFmr1 affects the piRNA pathway in the somatic and in the germline cells of the adult testes

We then assessed the tissue-specific requirement of *dFmr1* in the piRNA pathway that controls crystal formation. Germline-driven dFmr1 expression rescues the crystal phenotype of heterozygous $dFmr1^{\Delta 113}$ testes (Table 1, compare genotypes 21–23) and *c135-Gal4*-dependent *dFmr1* KD triggers crystal formation (Table 1, genotype 24). Thus, *dFmr1* works in the male germline, like all the so far identified members of the piRNA pathway controlling the *cry–Ste* interaction, including Aub [(Bozzetti et al., 2012; Ishizu et al., 2012; Nishida et al., 2007 and references therein]. We noticed that the *nos-Gal4* driven *dFmr1* KD does not trigger the crystal phenotype, even upon using two doses of the driver line (Table 1, genotypes 25,26). Upon closer inspection of the GFP-driven expression, we believe that the different behavior depends on the much earlier expression of the

Journal of Cell Science (2015) 128, 2070-2084 doi:10.1242/jcs.161810

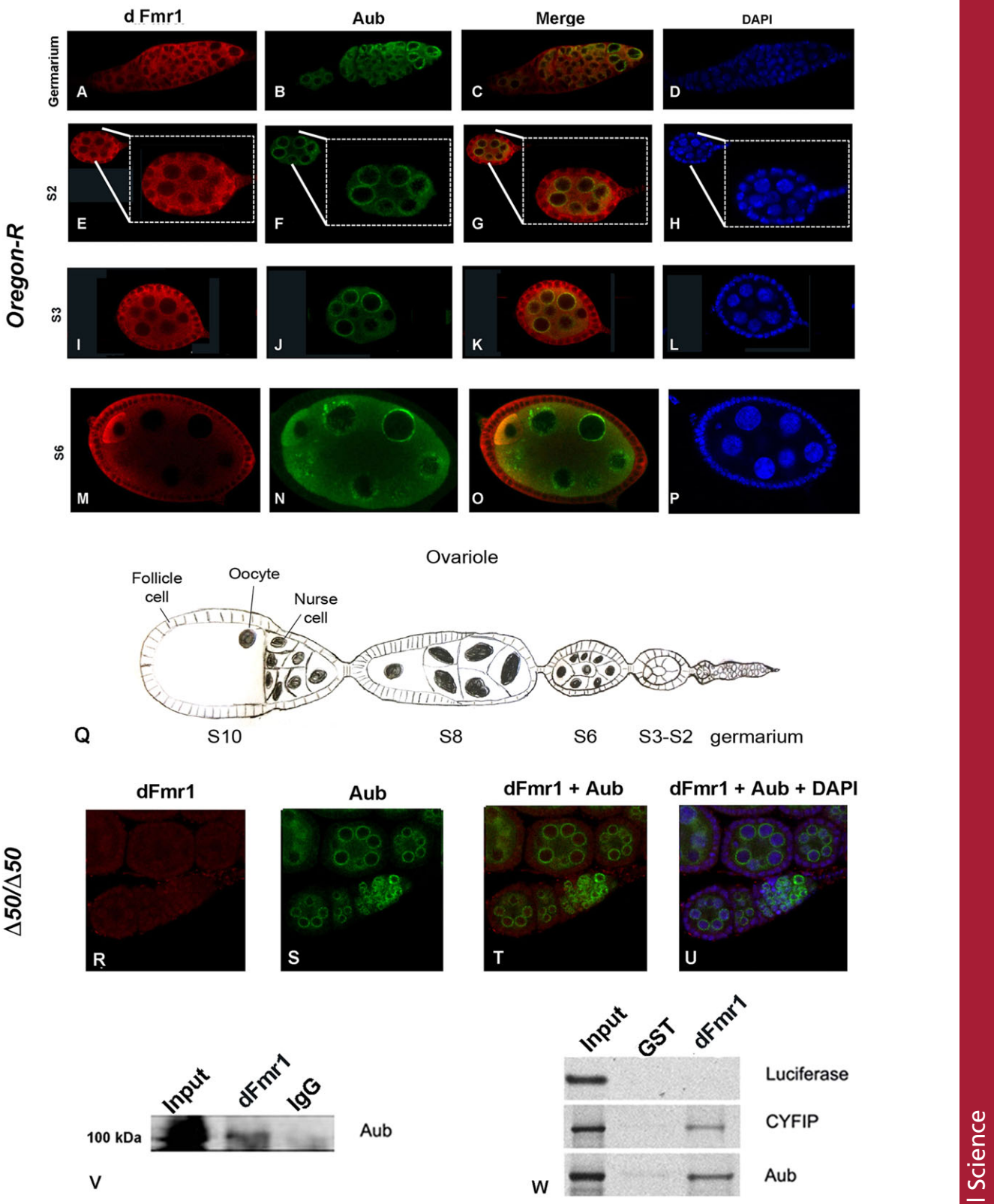

Fig. 4. dFmr1-Aub colocalization in ovaries. Projections of confocal sections from wt (A–P) or *dFMR1*$^{\Delta 50}$ homozygous ovaries (R–U). (Q) Schematic of an ovariole. Labeling was with anti-dFmr1 antibody (red, A,E,I,M,Q), anti-Aub antibody (green, B,F,J,N,R). The merged image is also shown (C,G,K,O,S). Blue, DAPI labeling (D,H,L,P). The triple labeling is shown in T. The images were taken with a 40× magnification objective. The inset in E–H shows a zoomed image of the (Stage 2) S2 ovary. (A–D) Note the Aub–dFMR1 colocalization in the germarium, which is highest at the level of the germ stem cell (right tip). (E–P) At later stages (S2–S6), the nuage around the nurse cell nuclei also shows overlap between Aub and dFmr1 and intense colocalization is observed in the oocyte cytoplasm (S6). In the mutant ovary (R–U), no dFmr1 labeling can be detected, as expected, and Aub is present and localizes at the nuage of the nurse cells as in the wt. (V) Co-immunoprecipitation of Aub with dFmr1 from S2 cells transiently transfected with full-length Aub and dFmr1 expression vectors. (W) Pulldown assay with *in vitro* translated dFmr1 and Aub. Luciferase was used as a negative control of interaction, CYFIP as a positive control (Schenck et al., 2003).

Journal of Cell Science (2015) 128, 2070-2084 doi:10.1242/jcs.161810

Table 1. 'Crystal' phenotypes in different genetic background

Genotypes	Crystals
1. *UAS-aub, dFmr1$^{\Delta 113}$/ nos-Gal4*	–
2. *T76-Gal4/+; UAS-aub, dFmr1$^{\Delta 113}$/+*	–
3. *UAS-aub, dFmr1$^{\Delta 113}$/c135-Gal4*	–
4. *UAS-dFmr1/+; UAS-aub RNAi/ c135-Gal4*	–
5. *UAS-dFmr1/+; UAS-aub RNAi/ nos-Gal4*	+
6. *UAS-aub RNAi / nos-Gal4/+*	+
7. *UAS-aub RNAi /c135-Gal4*	+
8. *upd-Gal4/Y; UAS-aub, dFmr1$^{\Delta 113}$/+*	–
9. *aub^{HN}/ +*	–
10. *aub^{QC42}/ +*	–
11. *aub^{HN}/ aub^{QC42}*	+
12. *aub^{HN}/ +; dFmr1$^{\Delta 113}$/+*	+
13. *aub^{QC42}/ +; dFmr1$^{\Delta 113}$/+*	+
14. *aub^{sting}/+*	–
15. *aub^{sting}/ aub^{HN}*	+
16. *aub^{sting}/ aub^{QC42}*	+
17. *aub^{sting}/ aub^{sting}*	+
18. *aub^{sting}/ +; dFmr1$^{\Delta 113}$/+*	–
19. *aub^{sting}/ +; dFmr1$^{\Delta 50}$/ dFmr1$^{\Delta 50}$*	–
20. *aub^{sting}/ +; dFmr1$^{\Delta 113}$/ dFmr1$^{\Delta 113}$*	–
21. *UAS-dFmr1/+; dFmr1$^{\Delta 113}$/c135-Gal4*	–
22. *UAS-dFmr1/+; dFmr1$^{\Delta 113}$/nos-Gal4*	–
23. *UAS-dFmr1/+; dFmr1$^{\Delta 113}$/+*	+
24. *UAS-dFmr1RNAi/ c135-Gal4*	+
25. *UAS-dFmr1RNAi/ nos-Gal4/+*	–
26. *UAS-dFmr1RNAi/+; nos-Gal4/ nos-Gal4*	–
27. *upd-Gal4/Y; UAS-dFmr1 RNAi/+*	+
28. *upd-Gal4/Y; UAS-dFmr1/ dFMR1$^{\Delta 113}$*	–
29. *upd-Gal4/Y; UAS-aub RNAi/+*	–
30. *upd-Gal4/Y; aub^{HN}/+; UAS-aub,dFmr1$^{\Delta 113}$/+*	+
31. *AGO1^{k08121}/+*	+
32. *AGO1 ^{04845}/+*	+
33. *AGO1^{k08121}/ AGO1^{04845}*	+
34. *upd-Gal4/Y; UAS-AGO1 RNAi/+*	+
35. *AGO1^{k08121}/aub^{sting}*	–
36. *AGO1^{04845}/aub^{sting}*	–

+, Crystals were present; –, crystals not present. For genotype 4, there was 1 escaper. None of the Gal4 lines, the UAS lines used for the overexpression assays or UAS RNAi lines exhibit crystals on their own.

nos-Gal4 compared to that of the *c135-Gal4* driver (supplementary material Fig. S3). This suggests that dFmr1 is required at a specific stage for the piRNA-mediated *cry–Ste* regulation.

The above data imply that dFmr1 protects from DNA instability in the germline. However, the rescue of the dFmr1-mediated crystal phenotype obtained with somatic Aub expression (*aub^{sting}* or with *upd-Gal4* driven expression) implies that this piRNA pathway also requires dFmr1 in somatic cells of the testis, directly or indirectly. This is also in line with the observation that 'somatic' transposons like *ZAM*, as well as 'germline' transposons are activated in *dFmr1* mutant animals (Fig. 2G,H). The formal demonstration that somatic dFmr1 accumulation directly affects the *cry–Ste* system, however, comes from the following assays: (1) *dFmr1* KD in the hub leads to the formation of crystals (Table 1, genotype 27; Fig. 7A), and (2) *dFmr1* expression driven by *upd-Gal4* rescues the crystal phenotype of *dFmr1* testes (Table 1, genotype 28; Fig. 7B). Of note, *aub* KD in the hub does not trigger crystal formation, further emphasizing the specificity of the *dFmr1*-mediated phenotype (Table 1, genotype 29). Thus, dFmr1 is required in the hub to suppress the formation of crystals in the male germline and high levels of somatic Aub or dFmr1 cause the recovery of the *dFmr1*-dependent crystal phenotype. Importantly, even though somatic Aub expression rescues the *dFmr1*-mediated crystal phenotype, this strictly depends on the endogenous Aub: somatic Aub expression no longer rescues the *dFmr1*-dependent crystal phenotype if the germline expression of Aub is lowered (Table 1, compare genotypes 28–30; Fig. 7C). Taken together, these results show that dFmr1 as well as Aub are required in the male germline to prevent crystal formation and dFmr1 is also required in the somatic cells of the male gonad. To the best of our knowledge, this is the first example of a case of a gene required in the hub to suppress crystal formation in the germline.

The dFmr1 larval synaptic phenotype is rescued by Aub somatic expression

The ability of ectopic Aub expression in the hub to rescue the *dFmr1* crystal phenotype led us to extend our analysis of this member of the piRNA pathway to another somatic tissue. Recent studies have documented the expression of piRNAs in the *Drosophila* nervous system and the occurrence of *aub*-dependent transposition in memory-relevant neurons in the brain (Lee et al., 2011; Perrat et al., 2013). Furthermore, small RNA and in particular piRNAs are involved in the epigenetic control of synaptic plasticity in Aplysia (Rajasethupathy et al., 2012). We hence turned our attention to

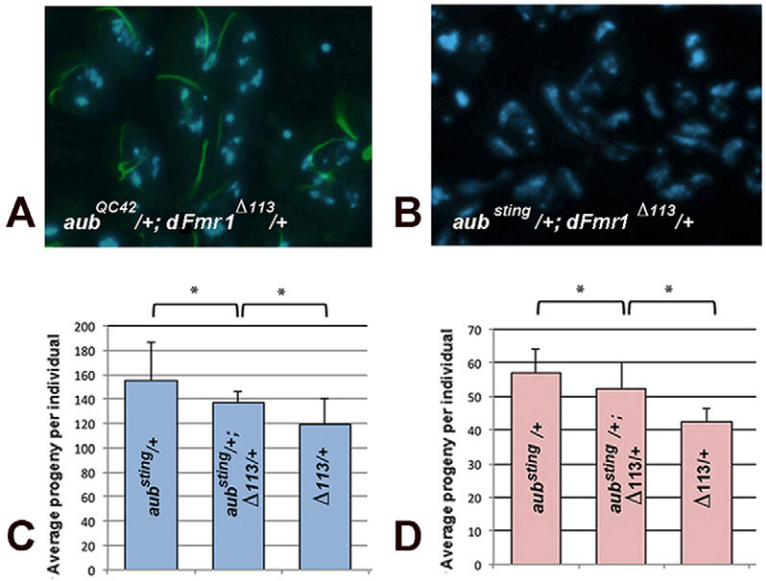

Fig. 5. Aub and dFmr1 interact genetically. (A,B) Crystal phenotype of the indicated genotypes. (C,D) Fertility of *dFmr1$^{\Delta 113}$* males (C) or females (D) and rescue by *aub^{sting}*. Results are mean±s.d. (n=3). *P<0.05.

Journal of Cell Science (2015) 128, 2070-2084 doi:10.1242/jcs.161810

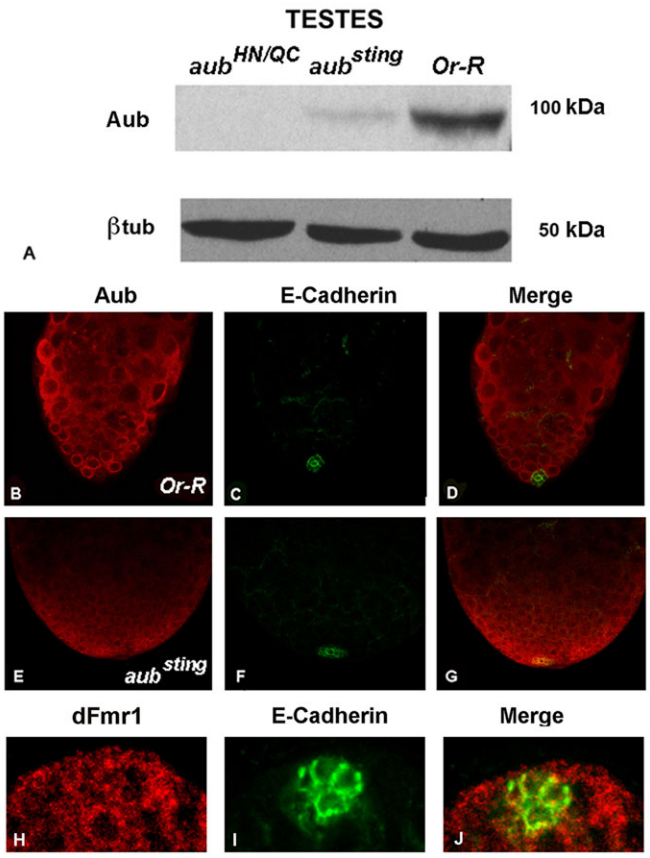

Fig. 6. Aub and dFmr1 expression in adult wt and mutant testes. (A) Western blot analysis with anti-Aub antibody in aub^{HN}/aub^{QC42}, aub^{sting} and *Or-R* (wt) testes. The lower panel shows the anti-β-tubulin antibody loading control. (B–G) Single confocal sections of wt testes (B–D) or aub^{sting} testes (E–G) labeled with anti-Aub antibody in red and anti-E-Cadherin antibody in green. D and G show the merge. The images were taken with a 40× magnification objective. (H–J) Single section showing the hub in wt testis labeled with anti-dFmr1 antibody in red (H) and anti-E-Cadherin antibody in green (I). The merged image is shown in J. The images were taken with a 63× magnification objective.

this process, which is tightly controlled by FMRP (Bassell and Warren, 2008). The fly larval neuromuscular junction (NMJ) represents the classical *Drosophila* model for synaptic plasticity and *dFmr1* larvae display NMJs that are longer than the wt ones (Zarnescu et al., 2005) (Fig. 7D, compare columns 1,5 and Fig. 7E,I).

Loss of Aub does not affect NMJ morphology (Fig. 7D, columns 1,2 and Fig. 7E,F) and Aub is not detectable in the larval somatic tissues (Fig. 7L), paralleling the fact that Aub is not detected nor required in the somatic tissue of the gonad. Interestingly, however, aub^{sting} induces ectopic Aub expression in the soma and affects the NMJs, which are extremely and moderately undergrown in homozygous and heterozygous animals, respectively (Fig. 7D, columns 3,4 and Fig. 7G,H,L). The NMJ phenotype was further confirmed by inducing the expression of Aub with the Actin-Gal4 driver (supplementary material Fig. S4 and data not shown). Finally, and most interestingly, aub^{sting} rescues the *dFmr1* phenotype, as seen in double mutant animals (Fig. 7D, columns 4–6 and Fig. 7H–J), showing that somatic Aub expression counteracts the *dFmr1* loss of function phenotype, as for the hub (the somatic part of the testis).

The mode of action of Aub and the overall role of the piRNA pathway in the brain is still under intense investigation. Typically Aub is not uniformly distributed in different areas of the brain and so neither is the level of transposition (Lee et al., 2011). To assess whether Aub is expressed below threshold levels in the somatic tissues of the larva and whether its impact onto the NMJ is only detected upon removing both Aub and dFmr1, we analyzed double heterozygous animals and found that the NMJs look identical to the wt ones (data not shown). These data confirm that Aub is neither expressed nor required at the NMJ.

One possible explanation for the above results is that Aub might directly or indirectly impact on the pathway of other AGO proteins acting on synaptic growth. Previous work has shown that AGO1 interacts genetically with dFmr1 at the NMJ, the double mutant aggravating the overgrowth phenotype observed in the *dFmr1* mutant animals (Coles et al., 2008). Thus, AGO1 seems to control NMJ growth negatively, as does the forced expression of Aub in the soma. We therefore tested whether the NMJ overgrowth due to the loss of AGO1 is rescued by expressing Aub in the soma and found that the NMJ of $AGO1^{k08121}/aub^{sting}$ double mutant animals are significantly shorter than those of $AGO1^{k08121}/+$ animals (Fig. 7K). Again, NMJs that lack one dose of Aub and one of AGO1 are similar to those that only lack one dose of AGO1, supporting the hypothesis that Aub does not play a significant role at the NMJ on its own (Fig. 7K).

DISCUSSION

Here, we show for the first time that dFmr1, a member of the FMRP protein family, is involved in the piRNA pathway controlling the *cry–Ste* system. This is the first protein that has been found to be required both in the hub and in the germline for the function of this pathway.

dFmr1 participates in the piRNA pathway

dFmr1 is a translational regulator and its role in the miRNA pathway is widely accepted (Cziko et al., 2009; Jin et al., 2004a; Jin et al., 2004b; Zarnescu et al., 2005). We here provide several lines of evidence that dFmr1 can be considered as a 'bona fide' member of the piRNA pathway that keeps repetitive sequences and transposons silenced (Brennecke et al., 2007; Vagin et al., 2006). First, *dFmr1* mutant testes display crystalline aggregates, as do other mutants of the piRNA pathway (Schmidt et al., 1999; Specchia et al., 2010; (Aravin et al., 2003; Brennecke et al., 2007; Nagao et al., 2010; Nishida et al., 2007). Second, the levels of *cry*-specific and transposon-specific piRNAs dramatically decrease in *dFmr1* mutant testes. Third, as a consequence of this decrease, the *Ste* RNA is produced and, in addition, transposons are expressed at higher levels than in wt animals. Fourth, *dFmr1* mutant animals display fertility defects, a phenotype shown by several mutations affecting the piRNA pathway. The fact that recent screens did not identify dFmr1 as a member of the somatic piRNA pathway could be due to the heterogeneous phenotypes observed with the somatic transposons (present work) and/or to the material used for those assays (Czech et al., 2013; Handler et al., 2013). The *cry–Ste* system thus proves very efficient for identifying new members of this important pathway.

The movement of transposable elements is one of the molecular causes of DNA instability and sterility (Brennecke et al., 2007; Khurana et al., 2011; Klattenhoff et al., 2007; Peng and Lin, 2013; Tamanini et al., 1997). Considering that human patients mutant for FMRP also display defects in male and female gonads (Sherman, 2000; Tamanini et al., 1997), it will be interesting to characterize the activity of transposons and repetitive sequences in the gonads of mice or humans that are mutant for the FMRP pathway, although there might be no observable defects in mammals

Journal of Cell Science (2015) 128, 2070-2084 doi:10.1242/jcs.161810

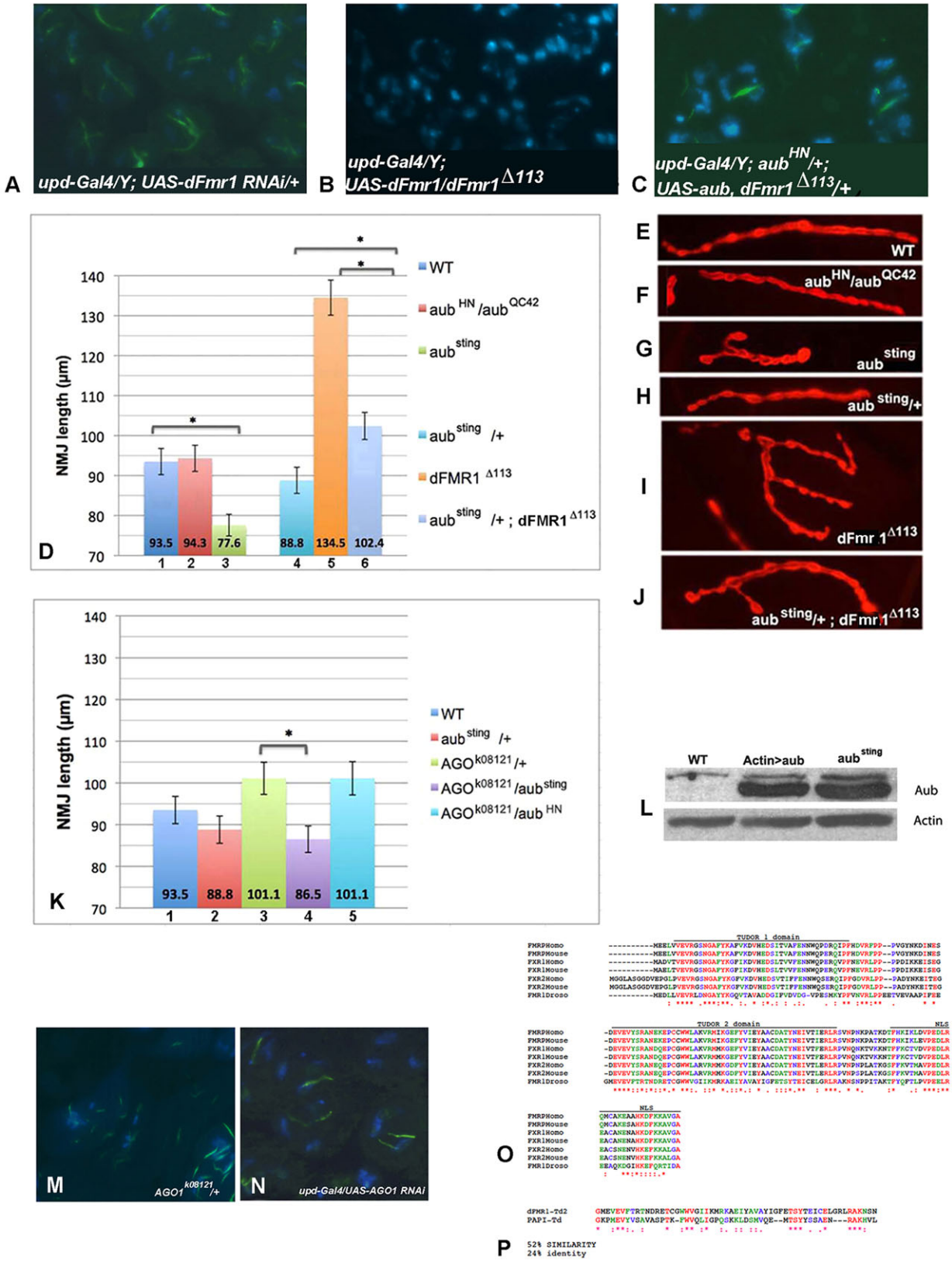

Fig. 7. See next page for legend.

because they express three members of the FMRP family versus the single ortholog in fly. Finally, we speculate that mutations affecting the piRNA pathway might also induce gonadal defects in humans.

dFmr1 and possible implications of the piRNA pathway in the somatic requirement

Until now, the members of the piRNA pathway controlling the *cry–Ste* interaction, including Aub, have been described as being required

Journal of Cell Science (2015) 128, 2070-2084 doi:10.1242/jcs.161810

Fig. 7. Germline and somatic requirements for dFmr1 in *cry–Ste* regulation, dFmr1–Aub genetic interactions in the nervous system and impact of AGO1 in testes. (A–C) Crystal phenotype of the indicated genotypes. (D) The mean±s.e.m. NMJ length (μm) of third-instar larvae (muscle 4, type Ib) of the indicated genotypes ($n \geq 60$). wt is w^{1118}, $dFmr1^{\Delta 113}$ is in homozygous conditions. (E–J) Representative NMJs of the mentioned genotypes (40×). (K) NMJ analysis of the indicated genotypes as in D. (L) Western blot on protein extracts from the third-instar larval carcasses of the mentioned genotypes. Actin was used as the loading control. (M,N) Crystal phenotypes of (M) $AGO1^{K08121}$/+ and (N) *upd-Gal4/UAS-AGO1 RNAi* testes. (O) Clustal alignment of human and mouse N-terminal of FMRP (FMRP Homo and FMRP Mouse, respectively), human and mouse Fragile-X related protein 1 and 2 (FXR1 and FXR2 Homo and Mouse, respectively), and *Drosophila* dFmr1 (FMR1 Droso). In red are the identical residues (asterisks), in blue the strongly similar residues (dots), in green the weakly similar residues (colons). The regions participating in the structure of the TDRDs are indicated as the TUDOR 1 and TUDOR 2 domains; the position of the nuclear localization signal is indicated (NLS). (P) Alignment of the TDRD2 of dFmr1 (amino acids 65–116) with the unique TDRD of PAPI (amino acids 258–307).

in the male germline (Brennecke et al., 2007; Cook et al., 2004; Klattenhoff and Theurkauf, 2008; Nagao et al., 2011; Pane et al., 2007). Surprisingly, the conditional *dFmr1* rescue and KD experiments demonstrate that dFmr1 controls the piRNA pathway both in the germline and in the somatic cells of the gonad, which raises questions as to the somatic contribution of other members of the piRNA pathway in the male gonad. The phenotypes induced by somatic Aub expression (Table 1, genotypes 8,18–20) also suggest that the hub expresses one or more AGO proteins that are involved in the somatic piRNA-mediated *Ste* silencing and that interact with dFmr1; however, the only other protein of the Piwi clade present in the somatic tissue, Piwi, does not participate in *Ste* silencing (Vagin et al., 2006). Based on preliminary data, we propose that AGO1 might be one such protein. First, *AGO1*/+ testes display Ste-made crystals (Table 1, genotypes 31–33; Fig. 7M,N), as do testes expressing *UAS-AGO1 RNAi* driven by the *upd-Gal4* driver (Table 1, genotype 34). Second, aub^{sting} rescues the *AGO1*-mediated crystal phenotype (Table 1, genotypes 35,36). Third, AGO1 and dFmr1 interact biochemically (Ishizuka et al., 2002) and are known to interact genetically in the ovaries to control germline stem cell maintenance, as well as in the nervous system, where they modulate synaptic plasticity (Bassell and Warren, 2008; Jin et al., 2004b). Taken together, these data suggest that AGO1 contributes to the piRNA pathway that controls the *cry–Ste* system in the somatic part of the gonad.

The finding that Aub somatic expression affects the NMJ and counteracts the *AGO1* loss of function phenotype was also unexpected. Recent work has documented the activation of piRNA pathway in the nervous system [in flies (Perrat et al., 2013), mice (Plaisant et al., 2008), humans (Lukic and Chen, 2011) and molluscs (Rajasethupathy et al., 2012)] and it has been proposed that synaptic plasticity, cognitive functions and neurodegeneration might involve the control of genome stability, even though the precise mode of action and impact of this pathway are not completely understood (Baillie et al., 2011; Lee et al., 2011; Li et al., 2013; Saxena et al., 2012; Tan et al., 2012). Because Aub is not required in the larval somatic tissues, its ectopic expression could affect the NMJ by replacing AGO1 in its known role on the miRNA pathway. However, AGO1 might also affect the NMJ through the piRNA pathway, much in the same way as *AGO1* loss of function affects a piRNA pathway in the gonad. Even though AGO1 has been previously described as being exclusively involved in the miRNA pathway, some degree of overlapping between different RNAi pathways has been recently described: (1) the double-stranded-RNA-binding protein Loquacious (Loqs) is involved in the miRNA pathway and in the endogenous siRNA pathway (Kim et al., 2009; Zhou et al., 2009), (2) AGO1 and AGO2 can compete for binding with miRNAs (Laskowitz and Warner, 2008), and (3) ectopic expression of Aub in the soma competes for the siRNAs pathway mediated by AGO2 (Specchia et al., 2008). In addition, miRNAs have been demonstrated to have a role on easi-RNA biogenesis in plants (Creasey et al., 2014). In a similar manner, AGO1 could act on piRNAs through its activity on the miRNA pathway. Although future studies will clarify the connection between AGO1 and the piRNA pathway, the present data provide novel perspectives in the field and could have a broad relevance to diseases affecting cognitive functions.

dFmr1 interacts with Aub

Our expression, genetic and biochemical data indicate that Aub and dFmr1 interact directly. dFmr1 has been proposed to bind specific cargo RNAs (Bassell and Warren, 2008; Dictenberg et al., 2008; Estes et al., 2008; Siomi et al., 1994; Siomi et al., 1995) and the human FMRP binds small RNA, in addition to mRNAs (Ascano et al., 2012b; Costa et al., 2005; Cziko et al., 2009; Jin et al., 2004b; Yang et al., 2009). Similarly, we speculate that the Aub–dFmr1 interaction allows the targeting of piRNAs to the transcripts of repetitive sequences and transposable elements, dFmr1 providing the molecular link between small RNAs and AGO proteins of the RISC.

The Aub and dFmr1 proteins colocalize and likely interact in the piRNA pathway in a specific stage of testis development and also have additional functions that are independent from each other. Typically, dFmr1 accumulates at high levels in more differentiated cells of the testis, where Aub is not detectable, likely accounting for the axoneme phenotype described in *dFmr1* testes (Zhang et al., 2004). In the future, it will be interesting to analyze whether the other genes involved in the piRNA pathway in testis are also required at specific stages, as also recently found in the ovary (Phillips et al., 2012).

Finally, FMRP proteins work in numerous molecular networks, show complex structural features (TUDOR, KH, NLS, NES RGG domains) and are characterized by widespread expression and subcellular localization (cytoplasm, nucleus, axons, dendrites, P bodies), providing versatile platforms that control mRNA and small RNA metabolism (e.g. translation, degradation and transport). Understanding whether FMRP proteins interact with other members of the piRNA pathway, whether this interaction is modulated physiologically and how does the interaction with this pathway compare with that observed with other AGO proteins will clarify the role and mode of action this family of proteins in small RNA biogenesis and metabolism.

The role of dFmr1 as a TUDOR protein

The biogenesis of the piRNAs requires two pathways. The primary pathway involves Piwi and predominantly occurs in the somatic tissues (Li et al., 2009; Malone et al., 2009). The ping-pong pathway involves Aub, as well as AGO3, and predominantly occurs in the germline, where Aub is thought to bind an antisense piRNA, to cleave the sense transcript from an active transposon and to produce a sense piRNA that is loaded onto AGO3 (Brennecke et al., 2007; Ishizu et al., 2012; Li et al., 2009; Malone et al., 2009; Nagao et al., 2010; Nishida et al., 2007). The AGO3–piRNA complex binds complementary transcripts from the piRNA cluster, producing the so-called secondary piRNAs by an amplification loop (Brennecke et al., 2007). Although the piRNA pathways have emerged as a very important tool to understand the role of RNA metabolism in physiological and pathological conditions, the relationship and interactions among the involved proteins are not simple to interpret,

Journal of Cell Science (2015) 128, 2070-2084 doi:10.1242/jcs.161810

mostly because not all the players have been characterized. Moreover, recent data support the hypothesis that the somatic and the germline piRNA pathways share components: for example, *shut down* (*shu*), *vreteno* (*vret*) and *armitage* (*arm*) affect primary as well as ping-pong pathways in ovaries (Olivieri et al., 2010; Saito et al., 2009). Our work calls for a role of dFmr1 in both piRNA pathways at least in testes. Based on the alignment of the human, mouse and fly FMRP family members, we speculate that dFmr1 participates to piRNA biogenesis as a Tudor domain (TDRD) containing protein (Maurer-Stroh et al., 2003) (Fig. 7O,P).

TDRDs are regions of about 60 amino acids that were first identified in a *Drosophila* protein called Tudor (Adams-Cioaba et al., 2010; Ramos et al., 2006; Siomi et al., 1994; Siomi et al., 1995). In the recent years, the requirement of TDRD proteins in piRNA biogenesis and metabolism has become evident (for a review, see Ishizu et al., 2012). Typically, the founding member of the family, Tudor, binds AGO proteins and helps them interact with specific piRNAs (Nishida et al., 2009). Among the different TDRD proteins, fs(1)Yb works in the primary pathway (Qi et al., 2011; Saito et al., 2010; Takata et al., 2008); Krimper, Tejas, Qin/Kumo, and PAPI work in the ping-pong pathway (Lim and Kai, 2007; Liu et al., 2011; Patil and Kai, 2010); and Vret works in both systems (Handler et al., 2011; Zamparini et al., 2011). PAPI, the only TDRD protein that has a modular structure closely related to dFmr1 (two KH domains and one TDRD), interacts with the di-methylated arginine residues of AGO3 and controls the ping-pong cycle in the nuage. At least during the early stages of testis development, dFmr1 might interact with Aub in a similar way. Given that TDRDs are involved in the interactions between proteins and in the formation of ribonucleoprotein complexes, future studies will assess whether RNAs mediate the Aub–dFmr1 interaction.

In conclusion, the discovery of dFmr1 as a player in the piRNA pathway highlights the importance of the fly model. Our data also add a new perspective to understanding the role and mode of action of this protein family and the physiopathological mechanisms underlying the Fragile X syndrome.

MATERIALS AND METHODS

Drosophila stocks

Flies were raised at 25°C on standard food. *Or-R* and w^{1118} flies were used as controls. All the stocks are described in FlyBase, as well as the expression profile of the drivers. They are listed in supplementary material Table S2.

We generated the *UAS-aub* vector and the transgenic line, which contains the complete AF 145680 coding sequence of the *aub* gene. We obtained *UAS-aub, dFmr1*$^{\Delta 113}$ flies by recombination.

Immunofluorescence of Ste-made crystals

Testes were dissected in Ringer's modified solution (182 mM KCl, 46 mM NaCl, 3 mM $CaCl_2$, 10 mM Tris-HCl pH 7.5). Testes were fixed with methanol, washed with PBST (1× PBS, 1% Triton X-100, 0.5% acetic acid) for 15 min, washed with 1× PBS for 5 min three times and incubated with the polyclonal mouse anti-Ste antibody (1:100) (Bozzetti et al., 1995). Samples were washed with 1× PBS for 5 min three times, incubated 2 h with 1:100 FITC-conjugated anti-mouse-IgG antibody (Jackson) and examined by epifluorescence microscopy (Nikon-Optiphot 2). Whenever necessary, DAPI was used at 100 ng/ml for nuclear labeling.

Northern blot analysis

An optimized protocol to detect small RNA analysis was employed (Pall and Hamilton, 2008). Total RNA extracted from freshly dissected testis cells was fractionated on 10% poly-acrylamide gel in MOPS–NaOH (pH 7), 7 M Urea and transferred onto Amersham Hybond-NX nylon membrane (GE Healthcare).

RNA cross-linking was performed, as described previously (Pall and Hamilton, 2008). DNA oligonucleotides complementary to the sequence of piRNAs *crystal, rasi4* and *R1* and to 5S rRNA were ^{32}P-labeled and used as probes. The sequences of the oligonucleotides are: *crystal*, 5′-UCGG-GCUUGUUCUACGACGAUGAGA-3′; *rasi4*, 5′-CGGUGUUCGACAG-UUCCUCGGG-3′; and *R1*, 5′-CUCGGAGUCCGACUCAGGAGAUCG-GA-3′.

The *crystal* piRNA corresponds to the that identified as *Su(Ste)-4* previously (Nishida et al., 2007); the *rasi4* piRNA corresponds to one of the most abundant crystal-related piRNA used previously (Specchia et al., 2010). The *R1* piRNA correspond to one of the piRNA related to *R1* identified previously (Nishida et al., 2007).

Total RNA extraction and qRT-PCR

Total RNA was extracted from 30 mg of male or female gonadal tissues using the RNAqueos-4 PCR Kit (AMBION) reagent following the manufacturer's protocol as described previously (Specchia et al., 2010). Samples were incubated with DNase I RNase free (AMBION) (1 Umg^{-1} RNA) at 37°C for 30 min (100 µl). DNase-treated RNA was precipitated at −80°C overnight and after centrifugation (10,000 ***g*** for 15 min) it was dissolved in 50 µl of nuclease-free water. The RNA concentration and purity were determined photometrically.

5 µg of total RNA were used as a template for oligonucleotide dT-primed reverse transcription using SuperScriptIII RNaseH-reverse transcriptase (Invitrogen), according to manufacturer's instructions. qRT-PCR was performed in the SmartCycler Real-time PCR (Cepheid) using SYBR green (Celbio) according to the manufacturer's protocol. For quantification of the transcripts, we used the $2\Delta\Delta C_t$ method as reported previously (Specchia et al., 2010). Primers are reported in supplementary material Table S3.

Male and female fertility testing

One young male was mated to three control virgin females, and three virgin females were mated with three control males. Ten individual males and 30 females were tested for each genotype. After 4 days, the crosses were transferred to a fresh vial. The parental flies were removed from the last vial after an additional 4 days. The number of the adult progeny from each vial was counted.

Statistical analysis

For comparisons between two measurements a two-tailed Student's *t*-test was used to show statistical significance.

Cell culture, transient transfection and western blot analyses

S2 cells were cultured in Schneider cell medium (Gibco BRL) plus 10% fetal calf serum. They were grown in monolayers at room temperature and transiently cotransfected with *pPAC-dFmr1* (Schenck et al., 2002) *pPAC-Gal4* and *pUAS-aub* vectors using Effectene reagent (Qiagen). S2 cells were scraped in Schneider cell medium and washed two times with 1× PBS. The pellet was resuspended in buffer A (400 mM KCl, 50 mM Tris-HCl pH 7.5, 20% glycerol, 5 mM DTT, 1 mM PMSF, 0.1% NP40 and 1× protease inhibitor cocktail) and cells were lysed by freeze and thaw three or four times. After adding three volumes of buffer A without KCl, the lysate was centrifuged at 12,000 ***g*** for 5 min. The precleaned supernatant (INPUT) was incubated with mouse anti-dFmr1 antibody [5A11, Developmental Studies Hybridoma Bank (DSHB)] for 2 h at 4°C and then with Protein-G–sepharose (GE Healthcare) overnight at 4°C. Beads were pelleted and the supernatant (SN) was saved for western blotting. After three washes in RIPA buffer, the beads were added to 1× Laemmli's loading buffer (50 mM Tris-HCl pH 6.8, 2% SDS, 100 mM dithiothreitol (DTT), 10% glycerol and 0.1% Bromophenol Blue]. The samples were boiled, pelleted and run on a 10% SDS-polyacrylamide gel. The gel was transferred at 250 mA onto a nitrocellulose membrane (Amersham). After blocking for 1 h in TBST (800 mM NaCl, 100 mM Tris-HCl pH 7.5, 0.1% Tween 20) with 5% dried milk powder, the membrane was incubated with rabbit anti-Aub antibody [Abcam or a gift from G. Hannon, Cold Spring Harbor Laboratory (CSH), New York] diluted 1:1000 in TBST plus 5% dried milk powder for 1 h at

room temperature or overnight at 4°C. The membrane was rinsed three times for 5 min in TBST followed by incubation for 1 h at room temperature with horseradish peroxidase (HRP)-conjugated anti-rabbit-IgG antibody (1:5000, Jackson). For western blot analysis, protein extracts were added to 2× Laemmli's loading buffer, boiled and run in a 10% SDS-polyacrylamide gel. For loading control, we used mouse anti-β-tubulin antibody (1:4000).

For gonadal extracts, testes were dissected in cold Ringer's solution (130 mM NaCl, 4.7 mM KCl, 1.9 mM $CaCl_2$, 10 mM Hepes pH 6.9) and mashed in lysis solution (50 mM NaCl, 50 mM Tris-HCl pH 7.5, 320 mM sucrose, 10% glycerol, 1% Triton X-100, and 1× protease inhibitor cocktail. They were centrifuged at 12,000 ***g*** for 10 min at 4°C. The amount of total protein was determined by Bradford assay.

For larval extracts, crude protein was extracted from carcasses of third-instar larval stage, in buffer (50 mM NaCl, 50 mM Tris-HCl pH 7.5, 10% glycerol, 320 mM sucrose, 1% Triton-X, Roche® protease inhibitor cocktail), from S2 cells in buffer (100 mM KCl, 20% glycerol, 50 mM Tris-HCl pH 7.5, 5 mM DTT, 1 mM PMSF, 0.1% NP40, Roche® protease inhibitor cocktail). After homogenization the samples were kept on ice for 10 min and centrifuged at 12,000 ***g*** for 10 min. Equal amounts of protein were loaded for SDS-PAGE on 8% gels. Each western blot was repeated three times.

Immunofluorescence of the whole gonads and confocal microscopy

Drosophila gonads were dissected in Ringer's solution and fixed with 4% paraformaldehyde for 20 min, washed with PBT (1× PBS with 0.5% Triton X-100), blocked with 5% NGS for 1 h and incubated with mouse anti-dFmr1 (1:300, DSHB), rabbit anti-Aub (1:300, gift from Brennecke), rabbit anti-Vasa (Santa Cruz Biotechnology), mouse anti-αSpectrin (DSHB), rat anti-E-Cadherin DHSB (1:100) antibodies at 4°C overnight. Samples were washed with PBST and then incubated for 2 h with the secondary antibodies against mouse IgG, rabbit IgG or goat IgG conjugated to FITC, Cy3 or Alexa Fluor® dyes (1:500, Jackson). All the samples were examined and captured using a laser-scanning confocal microscope (Zeiss LSM 700 on Axio imager M2).

GST pulldown assay

The Aub coding sequence was cloned in frame, using the following primers: 5′-ATGAATTTACCACCAAACCCTGT-3′, 5′-GTTAGCTGCGGCGTT-GTC-3′, 5′-GAACGCCTTCGCATGTTC-3′ and 5′-TTACAAAAAGTA-CAATTGATTCTGCAG-3′. Luciferase was used as negative control of the dFmr1 interaction and CYFIP as the positive control (Schenck et al., 2003). All are *in vitro* translated from the T3 and T7 promoters while radiolabeled with ^{35}S. GST tagged dFmr1 and GST alone overexpression was induced by 0.5 mM IPTG, 2 h at 37°C. Protein was purified as described before (de Santa Barbara et al., 1998). Purified GST and GST-dFmr1 were pulled down with *in vitro* translated proteins in 200mM NaCl containing buffer.

NMJ analysis

Dissection, antibody labeling of third-instar larvae and quantification of NMJ phenotypes were performed as described previously (Schenck et al., 2003). At least two rounds of independent assays were performed per genotype; for each round at least ten larvae of normal body size were dissected and 30 NMJs were analyzed for each assay. The synapse type-Ib on muscle 4, segments A2–A4 was analyzed. Pictures were taken at 40× with a of Zeiss Axiophot 2 microscope and imported in the in-house developed TCS/timt software that quantified synaptic length by automatic measurement. Statistical significance was calculated using ANOVA and the Newman-Keuls method for post hoc pair-wise analyses.

Acknowledgements

We thank J. Brennecke and G. Hannon for providing anti-Aub antibody; M. Van Doren and Y. Zhang for *Drosophila* strains; the Developmental Studies Hybridoma Bank and FlyBase for material and information. We thank O. F. Karatas and E. Green for sharing unpublished data as well as C. Delaporte and N. Arbogast for technical help.

Competing interests

The authors declare no competing or financial interests.

Author contributions

The work presented here was carried out in collaboration between the two laboratories. M.P.B. and A.G. defined the research plan and the strategies used in the paper, analyzed all the data, interpreted the results and wrote the paper. V.S. designed methods and experiments, carried out the confocal analysis of wild-type and mutant gonads, analyzed the data, interpreted the results and contributed to writing of the paper. P.B.C. designed, carried out and discussed some of the biochemical experiments. P.L. designed experiments and carried out the northern blotting analysis with the small RNAs. S.M. co-designed experiments with the antibodies and discussed the results. S.D.T. carried out some of the qRT-PCR experiments for the expression of transposons in wild-type and dFMR1 mutant animals. A.F. carried out western blotting analysis on testes and qRT-PCR. A.M.G. carried out the biochemical analysis and constructed some *Drosophila* lines used in the paper together with H.B.S. and C.D. H.B.S. co-designed the biochemical and somatic experiments and discussed the overall results, and also cloned the Aub constructs, performed the GST pulldown, the western blot analysis, dissected the wild-type and mutant larvae, carried out all the NMJ analysis and interpreted the results.

Funding

The work in the Giangrande laboratory was funded by the Institut National de la Santé et de la Recherche Médicale; Centre National de la Recherche Scientifique, Université de Strasbourg; Hôpital de Strasbourg; Association pour la Recherche sur le Cancer; Institut National du Cancer; Agence Nationale de la Recherche (ANR); Région Alsace; and the FRAXA foundation. It was also supported a French State fund managed by the Agence Nationale de la Recherche under the frame programme Investissements d'Avenir labeled ANR-10-IDEX-0002-02 [grant number ANR-10-LABX-0030-INRT]. H.B.S. was supported by the AFM, the FRM and the Région Alsace, A.M.G. by the FRAXA foundation, P.L. by the FRM, and P.C. by the ANR. V.S. acknowledges the grant from the MIUR for the project 'Futuro in ricerca 2010' [grant number RBFR10V8K6], as well as the EMBO for the short-term fellowship in 2009 to visit the lab of A.G. S.D.T. was supported by the MIUR [grant number PONa3_00334]. We also acknowledge the financial support of Telethon-Italy [grant number GG14181].

Supplementary material

Supplementary material available online at
http://jcs.biologists.org/lookup/suppl/doi:10.1242/jcs.161810/-/DC1

References

Adams-Cioaba, M. A., Guo, Y., Bian, C., Amaya, M. F., Lam, R., Wasney, G. A., Vedadi, M., Xu, C. and Min, J. (2010). Structural studies of the tandem Tudor domains of fragile X mental retardation related proteins FXR1 and FXR2. *PLoS ONE* **5**, e13559.

Anand, A. and Kai, T. (2012). The tudor domain protein kumo is required to assemble the nuage and to generate germline piRNAs in Drosophila. *EMBO J.* **31**, 870-882.

Aravin, A. A., Naumova, N. M., Tulin, A. V., Vagin, V. V., Rozovsky, Y. M. and Gvozdev, V. A. (2001). Double-stranded RNA-mediated silencing of genomic tandem repeats and transposable elements in the D. melanogaster germline. *Curr. Biol.* **11**, 1017-1027.

Aravin, A. A., Lagos-Quintana, M., Yalcin, A., Zavolan, M., Marks, D., Snyder, B., Gaasterland, T., Meyer, J. and Tuschl, T. (2003). The small RNA profile during Drosophila melanogaster development. *Dev. Cell* **5**, 337-350.

Arya, G. H., Lodico, M. J., Ahmad, O. I., Amin, R. and Tomkiel, J. E. (2006). Molecular characterization of teflon, a gene required for meiotic autosome segregation in male Drosophila melanogaster. *Genetics* **174**, 125-134.

Ascano, M., Hafner, M., Cekan, P., Gerstberger, S. and Tuschl, T. (2012a). Identification of RNA-protein interaction networks using PAR-CLIP. *Wiley Interdiscip. Rev. RNA* **3**, 159-177.

Ascano, M., Jr, Mukherjee, N., Bandaru, P., Miller, J. B., Nusbaum, J. D., Corcoran, D. L., Langlois, C., Munschauer, M., Dewell, S., Hafner, M. et al. (2012b). FMRP targets distinct mRNA sequence elements to regulate protein expression. *Nature* **492**, 382-386.

Baillie, J. K., Barnett, M. W., Upton, K. R., Gerhardt, D. J., Richmond, T. A., De Sapio, F., Brennan, P. M., Rizzu, P., Smith, S., Fell, M. et al. (2011). Somatic retrotransposition alters the genetic landscape of the human brain. *Nature* **479**, 534-537.

Bassell, G. J. and Warren, S. T. (2008). Fragile X syndrome: loss of local mRNA regulation alters synaptic development and function. *Neuron* **60**, 201-214.

Bozzetti, M. P., Massari, S., Finelli, P., Meggio, F., Pinna, L. A., Boldyreff, B., Issinger, O. G., Palumbo, G., Ciriaco, C., Bonaccorsi, S. et al. (1995). The Ste locus, a component of the parasitic cry-Ste system of Drosophila melanogaster, encodes a protein that forms crystals in primary spermatocytes and mimics properties of the beta subunit of casein kinase 2. *Proc. Natl. Acad. Sci. USA* **92**, 6067-6071.

Bozzetti, M. P., Fanti, L., Di Tommaso, S., Piacentini, L., Berloco, M., Tritto, P. and Specchia, V. (2012). The "Special" crystal-stellate system in Drosophila melanogaster reveals mechanisms underlying piRNA pathway-mediated canalization. *Genet. Res. Int.* **2012**, 324293.

Brennecke, J., Aravin, A. A., Stark, A., Dus, M., Kellis, M., Sachidanandam, R. and Hannon, G. J. (2007). Discrete small RNA-generating loci as master regulators of transposon activity in Drosophila. *Cell* **128**, 1089-1103.

Brennecke, J., Malone, C. D., Aravin, A. A., Sachidanandam, R., Stark, A. and Hannon, G. J. (2008). An epigenetic role for maternally inherited piRNAs in transposon silencing. *Science* **322**, 1387-1392.

Carmell, M. A., Xuan, Z., Zhang, M. Q. and Hannon, G. J. (2002). The Argonaute family: tentacles that reach into RNAi, developmental control, stem cell maintenance, and tumorigenesis. *Genes Dev.* **16**, 2733-2742.

Caudy, A. A., Myers, M., Hannon, G. J. and Hammond, S. M. (2002). Fragile X-related protein and VIG associate with the RNA interference machinery. *Genes Dev.* **16**, 2491-2496.

Coles, J. A., Martiel, J. L. and Laskowska, K. (2008). A glia-neuron alanine/ammonium shuttle is central to energy metabolism in bee retina. *J. Physiol.* **586**, 2077-2091.

Cook, H. A., Koppetsch, B. S., Wu, J. and Theurkauf, W. E. (2004). The Drosophila SDE3 homolog armitage is required for oskar mRNA silencing and embryonic axis specification. *Cell* **116**, 817-829.

Costa, A., Wang, Y., Dockendorff, T. C., Erdjument-Bromage, H., Tempst, P., Schedl, P. and Jongens, T. A. (2005). The Drosophila fragile X protein functions as a negative regulator in the orb autoregulatory pathway. *Dev. Cell* **8**, 331-342.

Creasey, K. M., Zhai, J., Borges, F., Van Ex, F., Regulski, M., Meyers, B. C. and Martienssen, R. A. miRNAs trigger widespread epigenetically activated siRNAs from transposons in Arabidopsis. *Nature* **508**, 411-415.

Czech, B. and Hannon, G. J. (2011). Small RNA sorting: matchmaking for Argonautes. *Nat. Rev. Genet.* **12**, 19-31.

Czech, B., Preall, J. B., McGinn, J. and Hannon, G. J. (2013). A transcriptome-wide RNAi screen in the Drosophila ovary reveals factors of the germline piRNA pathway. *Mol. Cell* **50**, 749-761.

Cziko, A. M., McCann, C. T., Howlett, I. C., Barbee, S. A., Duncan, R. P., Luedemann, R., Zarnescu, D., Zinsmaier, K. E., Parker, R. R. and Ramaswami, M. (2009). Genetic modifiers of dFMR1 encode RNA granule components in Drosophila. *Genetics* **182**, 1051-1060.

de Roodt, A. R., Lago, N. R., Salomon, O. D., Laskowicz, R. D., Neder de Roman, L. E., Lopez, R. A., Montero, T. E. and Vega Vdel, V. (2009). A new venomous scorpion responsible for severe envenomation in Argentina: Tityus confluens. *Toxicon* **53**, 1-8.

de Santa Barbara, P., Moniot, B., Poulat, F., Boizet, B. and Berta, P. (1998). Steroidogenic factor-1 regulates transcription of the human anti-müllerian hormone receptor. *J. Biol. Chem.* **273**, 29654-29660.

Dictenberg, J. B., Swanger, S. A., Antar, L. N., Singer, R. H. and Bassell, G. J. (2008). A direct role for FMRP in activity-dependent dendritic mRNA transport links filopodial-spine morphogenesis to fragile X syndrome. *Dev. Cell* **14**, 926-939.

Epstein, A. M., Bauer, C. R., Ho, A., Bosco, G. and Zarnescu, D. C. (2009). Drosophila fragile X protein controls cellular proliferation by regulating cbl levels in the ovary. *Dev. Biol.* **330**, 83-92.

Estes, P. S., O'Shea, M., Clasen, S. and Zarnescu, D. C. (2008). Fragile X protein controls the efficacy of mRNA transport in Drosophila neurons. *Mol. Cell. Neurosci.* **39**, 170-179.

Förstemann, K., Horwich, M. D., Wee, L., Tomari, Y. and Zamore, P. D. (2007). Drosophila microRNAs are sorted into functionally distinct argonaute complexes after production by dicer-1. *Cell* **130**, 287-297.

Gunawardane, L. S., Saito, K., Nishida, K. M., Miyoshi, K., Kawamura, Y., Nagami, T., Siomi, H. and Siomi, M. C. (2007). A slicer-mediated mechanism for repeat-associated siRNA 5′ end formation in Drosophila. *Science* **315**, 1587-1590.

Handler, D., Olivieri, D., Novatchkova, M., Gruber, F. S., Meixner, K., Mechtler, K., Stark, A., Sachidanandam, R. and Brennecke, J. (2011). A systematic analysis of Drosophila TUDOR domain-containing proteins identifies Vreteno and the Tdrd12 family as essential primary piRNA pathway factors. *EMBO J.* **30**, 3977-3993.

Handler, D., Meixner, K., Pizka, M., Lauss, K., Schmied, C., Gruber, F. S. and Brennecke, J. (2013). The genetic makeup of the Drosophila piRNA pathway. *Mol. Cell* **50**, 762-777.

Hillebrand, J., Barbee, S. A. and Ramaswami, M. (2007). P-body components, microRNA regulation, and synaptic plasticity. *ScientificWorldJournal* **7**, 178-190.

Hrdlicka, L., Gibson, M., Kiger, A., Micchelli, C., Schober, M., Schöck, F. and Perrimon, N. (2002). Analysis of twenty-four Gal4 lines in Drosophila melanogaster. *Genesis* **34**, 51-57.

Ishizu, H., Siomi, H. and Siomi, M. C. (2012). Biology of PIWI-interacting RNAs: new insights into biogenesis and function inside and outside of germlines. *Genes Dev.* **26**, 2361-2373.

Ishizuka, A., Siomi, M. C. and Siomi, H. (2002). A Drosophila fragile X protein interacts with components of RNAi and ribosomal proteins. *Genes Dev.* **16**, 2497-2508.

Jin, P. and Warren, S. T. (2000). Understanding the molecular basis of fragile X syndrome. *Hum. Mol. Genet.* **9**, 901-908.

Jin, P., Alisch, R. S. and Warren, S. T. (2004a). RNA and microRNAs in fragile X mental retardation. *Nat. Cell Biol.* **6**, 1048-1053.

Jin, P., Zarnescu, D. C., Ceman, S., Nakamoto, M., Mowrey, J., Jongens, T. A., Nelson, D. L., Moses, K. and Warren, S. T. (2004b). Biochemical and genetic interaction between the fragile X mental retardation protein and the microRNA pathway. *Nat. Neurosci.* **7**, 113-117.

Khurana, J. S., Wang, J., Xu, J., Koppetsch, B. S., Thomson, T. C., Nowosielska, A., Li, C., Zamore, P. D., Weng, Z. and Theurkauf, W. E. (2011). Adaptation to P element transposon invasion in Drosophila melanogaster. *Cell* **147**, 1551-1563.

Kibanov, M. V., Egorova, K. S., Ryazansky, S. S., Sokolova, O. A., Kotov, A. A., Olenkina, O. M., Stolyarenko, A. D., Gvozdev, V. A. and Olenina, L. V. (2011). A novel organelle, the piNG-body, in the nuage of Drosophila male germ cells is associated with piRNA-mediated gene silencing. *Mol. Biol. Cell* **22**, 3410-3419.

Kim, V. N., Han, J. and Siomi, M. C. (2009). Biogenesis of small RNAs in animals. *Nat. Rev. Mol. Cell Biol.* **10**, 126-139.

Klattenhoff, C. and Theurkauf, W. (2008). Biogenesis and germline functions of piRNAs. *Development* **135**, 3-9.

Klattenhoff, C., Bratu, D. P., McGinnis-Schultz, N., Koppetsch, B. S., Cook, H. A. and Theurkauf, W. E. (2007). Drosophila rasiRNA pathway mutations disrupt embryonic axis specification through activation of an ATR/Chk2 DNA damage response. *Dev. Cell* **12**, 45-55.

Krusiński, T., Laskowska, A., Ozyhar, A. and Dobryszycki, P. (2008). The application of an immobilized molecular beacon for the analysis of the DNA binding domains from the ecdysteroid receptor proteins Usp and EcR's interaction with the hsp27 response element. *J. Biomol. Screen.* **13**, 899-905.

Lasko, P. (2013). The DEAD-box helicase Vasa: evidence for a multiplicity of functions in RNA processes and developmental biology. *Biochim. Biophys. Acta* **1829**, 810-816.

Laskowitz, D. T. and Warner, D. S. (2008). The use of S100B as a biomarker in subarachnoid hemorrhage: clarity in its promise and limits. *Crit. Care Med.* **36**, 2452-2453.

Laskowski, C. A. and Hillhouse, G. L. (2008). Two-coordinate d9 complexes. synthesis and oxidation of NHC nickel(I) amides. *J. Am. Chem. Soc.* **130**, 13846-13847.

Lee, E. J., Banerjee, S., Zhou, H., Jammalamadaka, A., Arcila, M., Manjunath, B. S. and Kosik, K. S. (2011). Identification of piRNAs in the central nervous system. *RNA* **17**, 1090-1099.

Lee, E., Iskow, R., Yang, L., Gokcumen, O., Haseley, P., Luquette, L. J., III, Lohr, J. G., Harris, C. C., Ding, L., Wilson, R. K. et al.; Cancer Genome Atlas Research Network (2012). Landscape of somatic retrotransposition in human cancers. *Science* **337**, 967-971.

Li, C., Vagin, V. V., Lee, S., Xu, J., Ma, S., Xi, H., Seitz, H., Horwich, M. D., Syrzycka, M., Honda, B. M. et al. (2009). Collapse of germline piRNAs in the absence of Argonaute3 reveals somatic piRNAs in flies. *Cell* **137**, 509-521.

Li, W., Prazak, L., Chatterjee, N., Grüninger, S., Krug, L., Theodorou, D. and Dubnau, J. (2013). Activation of transposable elements during aging and neuronal decline in Drosophila. *Nat. Neurosci.* **16**, 529-531.

Lim, A. K. and Kai, T. (2007). Unique germ-line organelle, nuage, functions to repress selfish genetic elements in Drosophila melanogaster. *Proc. Natl. Acad. Sci. USA* **104**, 6714-6719.

Liu, L., Qi, H., Wang, J. and Lin, H. (2011). PAPI, a novel TUDOR-domain protein, complexes with AGO3, ME31B and TRAL in the nuage to silence transposition. *Development* **138**, 1863-1873.

Lukic, S. and Chen, K. (2011). Human piRNAs are under selection in Africans and repress transposable elements. *Mol. Biol. Evol.* **28**, 3061-3067.

Malone, C. D., Brennecke, J., Dus, M., Stark, A., McCombie, W. R., Sachidanandam, R. and Hannon, G. J. (2009). Specialized piRNA pathways act in germline and somatic tissues of the Drosophila ovary. *Cell* **137**, 522-535.

Maurer-Stroh, S., Dickens, N. J., Hughes-Davies, L., Kouzarides, T., Eisenhaber, F. and Ponting, C. P. (2003). The Tudor domain 'Royal Family': Tudor, plant Agenet, Chromo, PWWP and MBT domains. *Trends Biochem. Sci.* **28**, 69-74.

Muerdter, F., Guzzardo, P. M., Gillis, J., Luo, Y., Yu, Y., Chen, C., Fekete, R. and Hannon, G. J. (2013). A genome-wide RNAi screen draws a genetic framework for transposon control and primary piRNA biogenesis in Drosophila. *Mol. Cell* **50**, 736-748.

Nagao, A., Mituyama, T., Huang, H., Chen, D., Siomi, M. C. and Siomi, H. (2010). Biogenesis pathways of piRNAs loaded onto AGO3 in the Drosophila testis. *RNA* **16**, 2503-2515.

Nagao, A., Sato, K., Nishida, K. M., Siomi, H. and Siomi, M. C. (2011). Gender-specific hierarchy in nuage localization of PIWI-interacting RNA factors in Drosophila. *Front. Genet.* **2**, 55.

Nishida, K. M., Saito, K., Mori, T., Kawamura, Y., Nagami-Okada, T., Inagaki, S., Siomi, H. and Siomi, M. C. (2007). Gene silencing mechanisms mediated by Aubergine piRNA complexes in Drosophila male gonad. *RNA* **13**, 1911-1922.

Nishida, K. M., Okada, T. N., Kawamura, T., Mituyama, T., Kawamura, Y., Inagaki, S., Huang, H., Chen, D., Kodama, T., Siomi, H. et al. (2009). Functional

involvement of Tudor and dPRMT5 in the piRNA processing pathway in Drosophila germlines. *EMBO J.* **28**, 3820-3831.
Olivieri, D., Sykora, M. M., Sachidanandam, R., Mechtler, K. and Brennecke, J. (2010). An in vivo RNAi assay identifies major genetic and cellular requirements for primary piRNA biogenesis in Drosophila. *EMBO J.* **29**, 3301-3317.
Pall, G. S. and Hamilton, A. J. (2008). Improved northern blot method for enhanced detection of small RNA. *Nat. Protoc.* **3**, 1077-1084.
Palumbo, G., Bonaccorsi, S., Robbins, L. G. and Pimpinelli, S. (1994). Genetic analysis of Stellate elements of Drosophila melanogaster. *Genetics* **138**, 1181-1197.
Pane, A., Wehr, K. and Schüpbach, T. (2007). zucchini and squash encode two putative nucleases required for rasiRNA production in the Drosophila germline. *Dev. Cell* **12**, 851-862.
Patil, V. S. and Kai, T. (2010). Repression of retroelements in Drosophila germline via piRNA pathway by the Tudor domain protein Tejas. *Curr. Biol.* **20**, 724-730.
Pek, J. W., Patil, V. S. and Kai, T. (2012). piRNA pathway and the potential processing site, the nuage, in the Drosophila germline. *Dev. Growth Differ.* **54**, 66-77.
Peng, J. C. and Lin, H. (2013). Beyond transposons: the epigenetic and somatic functions of the Piwi-piRNA mechanism. *Curr. Opin. Cell Biol.* **25**, 190-194.
Perrat, P. N., DasGupta, S., Wang, J., Theurkauf, W., Weng, Z., Rosbash, M. and Waddell, S. (2013). Transposition-driven genomic heterogeneity in the Drosophila brain. *Science* **340**, 91-95.
Phillips, S., Stanley, L., Nicoletto, H., Burkman, M., Laskowitz, D. T. and Cairns, C. B. (2012). Use of emergency department transcranial Doppler assessment of reperfusion after intravenous tPA for ischemic stroke. *J. Emerg. Med.* **42**, 40-43.
Plaisant, C., Grinstein, G., Scholtz, J., Whiting, M., O'Connell, T., Laskowski, S., Chien, L., Tat, A., Wright, W., Görg, C. et al. (2008). Evaluating visual analytics at the 2007 VAST Symposium contest. *IEEE Comput. Graph. Appl.* **28**, 12-21.
Qi, H., Watanabe, T., Ku, H. Y., Liu, N., Zhong, M. and Lin, H. (2011). The Yb body, a major site for Piwi-associated RNA biogenesis and a gateway for Piwi expression and transport to the nucleus in somatic cells. *J. Biol. Chem.* **286**, 3789-3797.
Rajasethupathy, P., Antonov, I., Sheridan, R., Frey, S., Sander, C., Tuschl, T. and Kandel, E. R. (2012). A role for neuronal piRNAs in the epigenetic control of memory-related synaptic plasticity. *Cell* **149**, 693-707.
Ramos, A., Hollingworth, D., Adinolfi, S., Castets, M., Kelly, G., Frenkiel, T. A., Bardoni, B. and Pastore, A. (2006). The structure of the N-terminal domain of the fragile X mental retardation protein: a platform for protein-protein interaction. *Structure* **14**, 21-31.
Reeve, S. P., Bassetto, L., Genova, G. K., Kleyner, Y., Leyssen, M., Jackson, F. R. and Hassan, B. A. (2005). The Drosophila fragile X mental retardation protein controls actin dynamics by directly regulating profilin in the brain. *Curr Biol.* **15**, 1156-1163.
Reilly, M. T., Faulkner, G. J., Dubnau, J., Ponomarev, I. and Gage, F. H. (2013). The role of transposable elements in health and diseases of the central nervous system. *J. Neurosci.* **33**, 17577-17586.
Saito, K., Inagaki, S., Mituyama, T., Kawamura, Y., Ono, Y., Sakota, E., Kotani, H., Asai, K., Siomi, H. and Siomi, M. C. (2009). A regulatory circuit for piwi by the large Maf gene traffic jam in Drosophila. *Nature* **461**, 1296-1299.
Saito, K., Ishizu, H., Komai, M., Kotani, H., Kawamura, Y., Nishida, K. M., Siomi, H. and Siomi, M. C. (2010). Roles for the Yb body components Armitage and Yb in primary piRNA biogenesis in Drosophila. *Genes Dev.* **24**, 2493-2498.
Sato, K. and Siomi, H. (2010). Is canalization more than just a beautiful idea? *Genome Biol.* **11**, 109.
Saxena, A., Tang, D. and Carninci, P. (2012). piRNAs warrant investigation in Rett Syndrome: an omics perspective. *Dis. Markers* **33**, 261-275.
Schenck, A., Van de Bor, V., Bardoni, B. and Giangrande, A. (2002). Novel features of dFMR1, the Drosophila orthologue of the fragile X mental retardation protein. *Neurobiol. Dis.* **11**, 53-63.
Schenck, A., Bardoni, B., Langmann, C., Harden, N., Mandel, J. L. and Giangrande, A. (2003). CYFIP/Sra-1 controls neuronal connectivity in Drosophila and links the Rac1 GTPase pathway to the fragile X protein. *Neuron* **38**, 887-898.
Schmidt, A., Palumbo, G., Bozzetti, M. P., Tritto, P., Pimpinelli, S. and Schäfer, U. (1999). Genetic and molecular characterization of sting, a gene involved in crystal formation and meiotic drive in the male germ line of Drosophila melanogaster. *Genetics* **151**, 749-760.
Senti, K. A. and Brennecke, J. (2010). The piRNA pathway: a fly's perspective on the guardian of the genome. *Trends Genet.* **26**, 499-509.
Sherman, S. L. (2000). Premature ovarian failure in the fragile X syndrome. *Am. J. Med. Genet.* **97**, 189-194.
Siomi, H., Choi, M., Siomi, M. C., Nussbaum, R. L. and Dreyfuss, G. (1994). Essential role for KH domains in RNA binding: impaired RNA binding by a mutation in the KH domain of FMR1 that causes fragile X syndrome. *Cell* **77**, 33-39.
Siomi, M. C., Siomi, H., Sauer, W. H., Srinivasan, S., Nussbaum, R. L. and Dreyfuss, G. (1995). FXR1, an autosomal homolog of the fragile X mental retardation gene. *EMBO J.* **14**, 2401-2408.
Specchia, V. and Bozzetti, M. P. (2009). Different aubergine alleles confirm the specificity of different RNAi pathways in Drosophila melanogaster. *Fly (Austin)* **3**, 170-172.
Specchia, V., Benna, C., Mazzotta, G. M., Piccin, A., Zordan, M. A., Costa, R. and Bozzetti, M. P. (2008). aubergine gene overexpression in somatic tissues of aubergine(sting) mutants interferes with the RNAi pathway of a yellow hairpin dsRNA in Drosophila melanogaster. *Genetics* **178**, 1271-1282.
Specchia, V., Piacentini, L., Tritto, P., Fanti, L., D'Alessandro, R., Palumbo, G., Pimpinelli, S. and Bozzetti, M. P. (2010). Hsp90 prevents phenotypic variation by suppressing the mutagenic activity of transposons. *Nature* **463**, 662-665.
Stapleton, W., Das, S. and McKee, B. D. (2001). A role of the Drosophila homeless gene in repression of Stellate in male meiosis. *Chromosoma* **110**, 228-240.
Takata, K., Sheng, H., Borel, C. O., Laskowitz, D. T., Warner, D. S. and Lombard, F. W. (2008). Long-term cognitive dysfunction following experimental subarachnoid hemorrhage: new perspectives. *Exp. Neurol.* **213**, 336-344.
Tamanini, F., Willemsen, R., van Unen, L., Bontekoe, C., Galjaard, H., Oostra, B. A. and Hoogeveen, A. T. (1997). Differential expression of FMR1, FXR1 and FXR2 proteins in human brain and testis. *Hum. Mol. Genet.* **6**, 1315-1322.
Tan, H., Qurashi, A., Poidevin, M., Nelson, D. L., Li, H. and Jin, P. (2012). Retrotransposon activation contributes to fragile X premutation rCGG-mediated neurodegeneration. *Hum. Mol. Genet.* **21**, 57-65.
Thomas, C. A., Paquola, A. C. and Muotri, A. R. (2012). LINE-1 retrotransposition in the nervous system. *Annu. Rev. Cell Dev. Biol.* **28**, 555-573.
Thomson, T. and Lin, H. (2009). The biogenesis and function of PIWI proteins and piRNAs: progress and prospect. *Annu. Rev. Cell Dev. Biol.* **25**, 355-376.
Thomson, T., Liu, N., Arkov, A., Lehmann, R. and Lasko, P. (2008). Isolation of new polar granule components in Drosophila reveals P body and ER associated proteins. *Mech. Dev.* **125**, 865-873.
Tomari, Y., Du, T., Haley, B., Schwarz, D. S., Bennett, R., Cook, H. A., Koppetsch, B. S., Theurkauf, W. E. and Zamore, P. D. (2004). RISC assembly defects in the Drosophila RNAi mutant armitage. *Cell* **116**, 831-841.
Tritto, P., Specchia, V., Fanti, L., Berloco, M., D'Alessandro, R., Pimpinelli, S., Palumbo, G. and Bozzetti, M. P. (2003). Structure, regulation and evolution of the crystal-Stellate system of Drosophila. *Genetica* **117**, 247-257.
Vagin, V. V., Sigova, A., Li, C., Seitz, H., Gvozdev, V. and Zamore, P. D. (2006). A distinct small RNA pathway silences selfish genetic elements in the germline. *Science* **313**, 320-324.
Verkerk, A. J., Pieretti, M., Sutcliffe, J. S., Fu, Y. H., Kuhl, D. P., Pizzuti, A., Reiner, O., Richards, S., Victoria, M. F., Zhang, F. P. et al. (1991). Identification of a gene (FMR-1) containing a CGG repeat coincident with a breakpoint cluster region exhibiting length variation in fragile X syndrome. *Cell* **65**, 905-914.
Yang, Y., Xu, S., Xia, L., Wang, J., Wen, S., Jin, P. and Chen, D. (2009). The bantam microRNA is associated with drosophila fragile X mental retardation protein and regulates the fate of germline stem cells. *PLoS Genet.* **5**, e1000444.
Zamparini, A. L., Davis, M. Y., Malone, C. D., Vieira, E., Zavadil, J., Sachidanandam, R., Hannon, G. J. and Lehmann, R. (2011). Vreteno, a gonad-specific protein, is essential for germline development and primary piRNA biogenesis in Drosophila. *Development* **138**, 4039-4050.
Zarnescu, D. C., Jin, P., Betschinger, J., Nakamoto, M., Wang, Y., Dockendorff, T. C., Feng, Y., Jongens, T. A., Sisson, J. C., Knoblich, J. A. et al. (2005). Fragile X protein functions with lgl and the par complex in flies and mice. *Dev. Cell* **8**, 43-52.
Zhang, Y. Q., Bailey, A. M., Matthies, H. J., Renden, R. B., Smith, M. A., Speese, S. D., Rubin, G. M. and Broadie, K. (2001). Drosophila fragile X-related gene regulates the MAP1B homolog Futsch to control synaptic structure and function. *Cell* **107**, 591-603.
Zhang, Y. Q., Matthies, H. J., Mancuso, J., Andrews, H. K., Woodruff, E., III, Friedman, D. and Broadie, K. (2004). The Drosophila fragile X-related gene regulates axoneme differentiation during spermatogenesis. *Dev. Biol.* **270**, 290-307.
Zhang, Z., Xu, J., Koppetsch, B. S., Wang, J., Tipping, C., Ma, S., Weng, Z., Theurkauf, W. E. and Zamore, P. D. (2011). Heterotypic piRNA Ping-Pong requires qin, a protein with both E3 ligase and Tudor domains. *Mol. Cell* **44**, 572-584.
Zhang, F., Wang, J., Xu, J., Zhang, Z., Koppetsch, B. S., Schultz, N., Vreven, T., Meignin, C., Davis, I., Zamore, P. D. et al. (2012). UAP56 couples piRNA clusters to the perinuclear transposon silencing machinery. *Cell* **151**, 871-884.
Zhou, R., Czech, B., Brennecke, J., Sachidanandam, R., Wohlschlegel, J. A., Perrimon, N. and Hannon, G. J. (2009). Processing of Drosophila endo-siRNAs depends on a specific Loquacious isoform. *RNA* **15**, 1886-1895.